Università degli Studi di Napoli Federico II

FACOLTA' DI INGEGNERIA

Dipartimento di Ingegneria Chimica, dei Materiali e della Produzione
Industriale D.I.C.MA.P.I.

Dottorato di Ricerca in Ingegneria dei Materiali e delle Strutture

XXVIII ciclo

"The Role Of Nanopatterning In Cell

And Nuclear Mechanics."

Coordinatore

Prof. G. Mensitieri

Tutor   **Candidata**

Prof. P.A. Netti   *Anna Panico*

Table of Contents

ABSTRACT

Biophysical signals are known to influence cell fate and functions. In particular, topographic cues exert a direct control over focal adhesions positioning and cytoskeletal assemblies. Moreover, the nuclear envelope is directly connected to the cytoskeleton and actin generated stresses can directly impact on nuclear shape and gene matter configuration. However, how topographic patterns might influence the processes above or more generally, cellular and nuclear mechanics is still unclear. The goal of this work is to investigate how the microenvironmental conditions in terms of topographic cues, substrate chemistry and cell-cell contacts may alter the cell morphology, along with cellular and nuclear mechanics. In a first set of experiments we used nanopatterned polydimethylsiloxane (PDMS) as cell culturing substrates. The patterns consisted of parallel and straight channels having ridge to groove width ratio of 1:1. Pattern features used were 700nm or 350 nm wide with depth of 250nm or 100nm respectively. Additionally, the chemistry of the material surface was modified by performing different functionalization treatments, namely fibronectin or serum coating. Mesenchymal Stem Cells (hMSC) were cultured at low densities on the substrates up to 48h. Atomic Force Microscopy (AFM) was employed to generate elasticity maps of the whole cell body. We then correlated local elastic modulus with cell height in order to discriminate the different cellular regions. Our analysis showed structural and mechanical heterogeneity of the cell body, clearly mediated by topographic and adhesive signal. In particular, the spindle like phenotype observed on the nanopatterned materials generates compressive forces on the nucleus, which increase its mechanical properties. Our results also demonstrated a positive correlation between the expression of lamins A / C, the structural proteins of the nucleus, and the mechanical properties of the nuclear region. Therefore it is reasonable to hypothesize that these proteins have a primary role in dictating the mechanical properties of the nucleus. In a second setup, we used endothelial cells (HUVECs) on flat PDMS substrates to investigate the effect of cell-cell contacts on cytoskeletal assembly and nuclear mechanics. We found that actin is redistributed in the cortical area, freeing the nucleus, which exhibits a mechanical conformation characterized by lower moduli than single cells. Our results pave the way for capturing designing concept to fabricate novel patterned platforms that effectively alters nuclear mechanics and possibly cell fate by tuning the material-cytoskeleton-nucleus crosstalk.

CHAPTER 1

INTRODUCTION

The fundamental studies of molecular biology were essentially focused on the effect of soluble signals on the cell fate and functions. The effect of non-biochemical signals but biophysical cues has been widely underestimated; only in the very recent past, it was demonstrated that the biophysical features of the extracellular space, where the cell resides, are as powerful as the biochemical ones. A landmark study by Engler et al. in 2006 showed that the mechanical properties of the culturing substrate can direct stem cell fate without using soluble factors [1]. Human stem cells were cultured on materials with a stiffness comparable to that of brain, muscle or bone and it was observed that the different substrates promoted neurogenesis, myogenesis and osteogenesis, respectively. From Engler's work on, many other studies have emerged on the development of artificial platforms for the control of cell fate. Several research activities have been carried out, through different approaches, with the common purpose of altering the cell contractility, the adhesive processes and the cytoskeleton architecture. In this context, Kilian et al. created adhesive patterns able to induce growing levels of contractility in human mesenchymal stem cells, i.e., blunt curves vs. sharp corners and rectangles with different aspect ratios [2]. They suggested that adhesive shapes promoting myosin-driven contractility, such as pointed stars or stretched rectangles, enhanced osteogenesis, whereas adhesive shapes in the form of round flowers or small squares induced little cell contractility and promoted adipogenesis. By following a different approach, Dalby et al. demonstrated that topographic patterns stabilizing intracellular tension promoted osteogenesis; conversely, patterns that promoted little contractile phenotype are requested to maintain multipotency [3,4]. Therefore, the paradigm of maximizing adhesion might provide unwanted affects. Generally

speaking adhesiveness should be sufficiently high to maintain cell viability, whereas small variation from that level may elicit very different cell responses. However how the cell translates adhesive and contractile signals in biochemical events is currently scarcely known. The transduction of exogenous signals, i.e., mechanical cues, in biochemical signals can occur at focal adhesions level, a cluster of integrins, that mediate the binding between the cell and the extracellular space. It is known that signaling proteins are embedded in focal adhesions, tyrosine kinase, i.e., Src and FAK that can be phosphorylated and then switched on. These, in turn, can activate other mechanotransductive pathways [5]. This process is referred to as an adhesion-mediated mechanotransduction. However, other mechanotransductive mechanisms linked to contractility processes were brought to light. For instance, McBeath et al. demonstrated that, by cultivating human stem cells on adhesive islands, the cell area was a determinant of cell differentiation as small islands promoted adipogenesis, whereas larger islands osteogenesis [6]. Furthermore, the authors suggested that cell contraction was involved in lineage specification through the RhoA/ROCK pathway, as direct manipulation of RhoA modulated adipogenesis/osteogenesis. Furthermore, a direct mechanotrasductive process can occur due to the actin network that alter the nuclear shape and stress state. In fact, the intracellular stress state dictated by the cytoskeleton architecture modulates nuclear mechanics. In this context, Isermann et al. showed that these processes have an effect on chromatin configuration at the nuclear level [7]. They suggested how force-induced nuclear deformation could modulate expression of mechano-responsive genes. Therefore, the role of biophysical features is of crucial relevance to govern the adhesive and contractile cellular processes and differentiation mechanisms.

These material-induced cell responses can have remarkable applications in the biomedical field, such as regenerative medicine. In this context, it can keep an

undifferentiated stem cell pool for a long time or controlling their differentiation in vitro in order to achieve an adequate ad purified cell population for cell therapies, scaffold seeding, or to realize devices for in vitro studies in which the combined effect of a soluble and a mechanical signal can be assessed. Additionally, a drug or a growth factor that read two different mechanical cues or topographies, can in principle elicit two totally different behaviors, and this process can be relevant in the context of drug discovery or screening.

On the basis of these concepts, here we investigated how different cytoskeletal assembly mediated by material features alters the stress state of the cytoplasmic and nuclear region, given the relevance of the contractility and nuclear shape in the cell differentiation. Between the various signals, we chose topographic patterns since these best suited for this purpose: topographic signals are stable and can exert a direct control over the positioning of the focal adhesions and the cytoskeleton structure through the well-known phenomenon of the contact guidance. This process shows that submicrometric pattern, i.e. nanopatterns, guide and confine the focal adhesion growth along the ridge of the pattern surface and not inside the groove. Thus, FA confinement leads to a preferred orientation of the actin cytoskeleton and the intracellular stress state. Conversely, on the flat substrates, without topography is harder to orchestrate these processes in a predetermined way [8]. For our purpose, two different topographic patterns, in form of parallel gratings, were produced and two various surface treatments were carried out in order to control the adhesiveness. Particular relevance in the context of mechanotransduction is given to stimuli able to dictate the differentiation of stem cells. Therefore, the cells employed in the first part of these studies are the mesenchymal stem cells, which represent a good model for single cell studies. To characterize the intracellular stress state we chose the atomic force microscopy, a high-resolution non-invasive technique, that allows to generate elasticity maps of

the whole cell body [9]. Then, in order to discriminate the two areas of interest, the cytoplasmic and nuclear region, we correlated local elastic modulus with cell height. Then, to better understand which structure really dictates the nuclear mechanics, we correlated the mechanical properties of the nuclear area with the expression of lamins A/C, structural proteins of the nuclear envelope and with the chromatin densification level.

We then investigated how cytoskeleton architecture and nuclear mechanics are connected in case of cell populations in presence of extensive cell-cell contacts. Here, we removed the topography and only flat substrates were employed for the experiments, but in this case we changed the cell density. Indeed, in any application context such as regenerative medicine or in vitro devices, single – cell investigations can be crucial to analyze given intracellular pathways but are not very useful for a practical translation where a high number of cells is required. Therefore, we used a suitable model for this type of study represented by the endothelial cells, which live naturally at high density. For our purpose, we studied the effect of cell – cell contact, mediated by Ve-Cadherin, on the actin cytoskeletal network with high resolution microscopy and then on the intracellular stress state in the cytoplasmic and nuclear region.

References

1. Engler AJ, Sen S, Sweeney HL, Discher DE. 2006 Matrix Elasticity Directs Stem Cell Lineage Specification. Cell. 126, 677–689.

2. Kilian KA, Bugarija B, Lahn BT, Mrksich M. 2010 Geometric Cues for Directing the Differentiation of Mesenchymal Stem Cells. Proc. Natl. Acad. Sci. U. S. A., 107, 4872–4877.

3. Dalby MJ, Gadegaard N, Tare R, Andar A, Riehle MO, Herzyk P, Wilkinson CD, Oreffo RO. 2007 The Control of Human Mesenchymal Cell Differentiation Using Nanoscale Symmetry and Disorder. Nat. Mater. 6, 997–1003.

4. McMurray RJ, Gadegaard N, Tsimbouri PM, Burges KV, McNamara LE, Tare R, Murawski K, Kingham E, Oreffo RO, Dalby MJ. 2011 Nanoscale Surfaces for the Long-Term Maintenance of Mesenchymal Stem Cell Phenotype and Multipotency. Nat. Mater. 10, 637–644.

5. Dalby MJ, Gadegaard N, Oreffo ROC. 2014 Harnessing nanotopography and integrin–matrix interactions to influence stem cell fate. Nature materials. 13, 558–569 doi:10.1038/nmat3980.

6. McBeath R, Pirone DM, Nelson CM, Bhadriraju K, Chen CS. 2004 Cell Shape, Cytoskeletal Tension, and RhoA Regulate Stem Cell Lineage Commitment. Dev. Cell, 6, 483–495.

7. Isermann P, Lammerding J. 2013 Nuclear Mechanics and Mechanotransduction in Health and Disease. Current Biology 23, R1113-R1121.

8. Natale CF, Ventre M, Netti PA. 2014 Tuning the Material-Cytoskeleton Crosstalk via Nanoconfinement of Focal Adhesions. Biomaterials, 35, 2743–2751.

9. Nikolaev N, Müller T, Williams DJ, Liu Y. 2014 Changes in the stiffness of human mesenchymal stem cells with the progress of cell death as measured by atomic force microscopy. Journal of Biomechanics 47 625–630.

CHAPTER 2

CELL MECHANICS: MEASUREMENT AND OPTIMIZATION OF THE EXPERIMENTAL SET-UP

The investigation of the mechanical properties of cells has been the subject of numerous scientific studies. The mechanical behavior of individual cells is strictly linked to their intracellular components, especially by the actin cytoskeleton [1,2]. Indeed, through the transmembrane integrins, the cytoskeleton and the nucleus, the cells transform mechanical cues into biochemical signals through mechanotransduction pathways. It has been shown, that significant alterations in the mechanical properties of the nucleus are related to fundamental biological processes, such as differentiation [3]. To achieve full understanding of the cell mechanical characterization theoretical models and specific experimental techniques have been developed. The ability to measure and analyze the cellular mechanical properties on relevant metric scales is born in conjunction with the development of new technologies originally aimed at determining the physico-morphological features of material surfaces. A large number of techniques for the measurement of cellular mechanical properties have been developed. These can be classified into two categories: techniques that rely on the application of forces and controlled deformation over the whole cell, or on parts of it such as Multi Particle Tracking, Magnetic and Optical Tweezers or the Atomic Force Microscopy (AFM), and others that monitor the ability of the cell and generate forces to change the surrounding environment [4].

The Particle Tracking Microrheology (PTM) allows to carry out localized measurements of cytoplasmic mechanical properties identifying the thermal induced movement of fluorescent markers into the cell, without the need of a direct

connection between cell surface and an external probe. Therefore, this contac-less technique also allows studying the mechanics of cells that are housed in three-dimensional matrices. In several experiments, the use of PTM on the cells revealed the existence of an elastic response in short observation times and a viscous regime in the long term. The Brownian motion of the markers within viscoelastic materials is related to the mechanical properties through the generalized Stokes-Einstein relation:

$$G^*(\omega) = \frac{k_B T}{i\omega \langle \Delta r(\omega)^2 \rangle \pi a}$$

Where α is the marker radius, k_B is the Boltzman constant, T is the absolute temperature, $[\Delta r(\omega)^2]$ is the Fourier transform of the mean square displacement of the particle, i is the imaginary unit and ω is the pulsation.

Because the term $[\Delta r(\omega)^2]$ represents a complex function, $G^*(\omega)$ also will be, in turn, a complex quantity; in particular the real part of the shear modulus, $G'(\omega)$ represents the linear elasticity modulus, while the imaginary part, $G''(\omega)$ is the dissipative modulus [5].

Additionally, the interaction between the particles integrated into the cell and the elastic network seems to be a major source of fluctuations in non-Brownian motion of the particles.

A second technique is the Magnetic Tweezers. A simple clamp (Magnetic Tweezers) is made up by a pair of permanent magnets, placed above the sample holder of an inverted microscope. The clamps are able to exert forces with intensity exceeding 1 nN, and can be used to rotate the magnetic particles of nano and micrometric size. A magnetic particle immersed in an external magnetic field can undergo a force proportional to the gradient of the square of the magnetic field. Because of the gradient is particularly steep, however, the force decreases rapidly with distance

from the source of the field. Consequently, forces of appreciable intensity will be applied to those particles that are also close to magnets [6].

This technique, unlike MPT, enables to lead direct measurements of the mechanical properties of nuclei in situ, through the arrangement of the magnetic particles at the nuclear membrane. The forces exerted by the magnetic particles at the nucleus do not cause an extensive deformation of the structure and therefore the analysis might be difficult to perform [7].

Young's modulus of a cell or subcellular comportments can be evaluated with atomic force microscopy (AFM). This is a technique of surface scanning with high spatial resolution, characterized by high versatility since it can be used in various environmental conditions, such as tissues, cells and even single molecules [8].

An atomic force microscope is equipped with a detection mechanism consisting of a cantilever, provided with a pointed end, said tip, of micrometric size. A piezoelectric actuator places the tip at the sample to be analyzed. During a scan, the interactions between the tip and sample induce deformation of the cantilever, which can be measured to reproduce the topography of the area subjected to analysis and to investigate their mechanical properties [9].

To extract the parameters of the cell elasticity, the tip of the cantilever is pressed on the surface of the cell, while it measures the deformation and the magnitude of the applied force. Once the geometry of the tip is known, it is possible to extrapolate the elastic properties of the cell (stiffness, Young's modulus) by means of the indentation depth as a function of the measured force and an appropriate analysis model [4,9]. The indentation-force relationship is most conveniently represented by a curve obtained by experimental data. In such curves, the contact point is defined as the onset of deformation (at zero force). If the sample is undeformable, the tip, after the contact with the surface, ends its descent and inclination of the cantilever will be equal to its vertical displacement. On the contrary, if the material is soft, the

tip will penetrate into the sample and the inclination of the cantilever will be lower than its vertical displacement. The value of Young's modulus can be determined by fitting a curve of indentation using the theoretical model of Hertz-Sneddon [9]. The Hertzian model describes the elastic penetration of a sample of infinite length by an indenter of simple geometric shape. The mathematical expression that underlies the force-distance curve is:

$$z = z_0 + \frac{F}{k} \sqrt{\frac{F(1-v^2)}{\frac{2}{\pi} E \tan(\alpha)}}$$

Where z is the displacement of the cantilever, z_0 is the position of the contact point, F is the force exerted by the cantilever, K is the spring constant of the cantilever, v is the Poisson's ratio, α is the angle of half-opening dell' indenter (hired as conical) and E is the Young's modulus [10]. It is possible to characterize the cell mechanics through the use of atomic force microscopes with modified tips in the form of fine needles. These tips penetrate into the cell resulting in the least possible damage to cell structures. This approach could also be applied to cells inserted into three-dimensional matrices, in order to better understand the mechanisms underlying the mechanobiology. It also allows to evaluate how nuclear mechanics affects cell development and functions [7]. The assessment of material mechanical properties by means of AFM is not direct, but relies on the use of theoretical models, i.e. Hertz-Sneddon, that are valid under stringent circumstances. For instance, the material should be linearly elastic and edge effects should be negligible. Living cells are far from these hypotheses. This notwithstanding, Hertz-Sneddon models are those most used to determine cell mechanical properties. The stress-strain curves have a non-linear behavior in consequence of the greater stiffness of the nuclear region compared to the cytoplasm. In fact, in correspondence of indentation depth larger

than 200 nm, the rigid nucleus affects to a greater extent on the deformation with respect to the membrane and the cell cortex. Because of the heterogeneous nature and the complexity of the cell cytoskeleton, micro and nano-scale measurements could lead to results substantial differences of mechanical properties. Given its complex hierarchical structure, the cells exhibit position-dependent force-deformation responses [4].

Aim of this work is to alter cell mechanical properties through surface mediated adhesion events. To achieve this goal, one has to deal with 1. non-ideality of cells, as materials whose properties fulfill Hertzian requirements; 2. Intrinsic heterogeneity of mechanical properties of individual cells. This requires to develop a robust procedure to extract and analyze data, thus drawing out statistically relevant conclusions. In more detail, in this chapter we reveal the technique used to detect the cellular stress state, or rather the mechanical properties of the cell, then we display the experimental set up optimization with the careful data processing and data cleaning. For this purpose, we employed nanopatterned substrates with 700nm wide ridge and groove and a control flat surface. In order to elicit specific cellular responses we controlled cell adhesion through two types of surface treatments. Samples were incubated with serum- supplemented culture medium (10%) or a fibronectin solution (10μg/mL). In this way modulated the adhesiveness since the fetal bovine serum solution contains a series of proteins that are not as effective as pure FN in promoting the cellular adhesion. Human MSC were used as relevant model to study mechanotransduction processes.

2.1. MATERIALS AND METHODS

2.1.1. Substrate Preparation

Patterned substrates were obtained by replica molding of polydimethylsiloxane (PDMS, Sylgard184) on a polycarbonate master. Two different substrates were fabricated in this experimental campaign: a nanograting and a flat substrate. Nanopatterned substrates containing parallel and straight channels having a ridge to groove width ratio of 1:1, with 700nm wide ridges and 700nm wide grooves and a depth of 250 nm. PDMS was prepared by mixing elastomer base and curing agent at a 10:1 weight ratio. PDMS solution was degassed, poured onto the polycarbonate master and then cured at 37 °C for 24 h. Flat substrates were produced by pouring the base and curing mix on a 35 mm polystyrene Petri dish (Corning) and curing at 37 °C for 24 h.

2.1.2. Functionalization of Substrates

Substrate adhesivity was altered through two types of functionalization. All PDMS samples were treated with oxygen plasma for 1 min and then incubated with either serum-supplemented culture medium at 37 °C or fibronectin (Fibronectin from Human Plasma, Sigma) solution at 4 °C (10 μg/ml) overnight prior to cell seeding.

2.1.3. Cell Culture

Human Mesenchymal Stem Cells (hMSCs) were cultured on functionalized surfaces in α-MEM (Modified Eagle's Medium, Lonza) supplemented with 10 % fetal bovine serum (FBS, Euroclone), 100 mg/ml L-glutamine, 100 U/ml penicillin/streptomycin

(Sigma). The cells were incubated in a humidified atmosphere at 37 °C and 5% CO_2 for 48h. Finally, samples were moved to the AFM holder for acquisitions.

2.1.4. AFM Experiment

Rectangular maps of force-distance curves were acquired per each cell in contact mode with an atomic force microscope JPK NanoWizard II (JPK Instruments). Before recording the map 1, the AFM tip was calibrated to evaluate the spring constant through the thermal noise method. This method relies on measuring the thermal fluctuations in the deflection of the cantilever, and using the equipartition theorem to relate this to the spring constant. Essentially, the thermal energy calculated from the absolute temperature should be equal to the energy measured from the oscillation of the cantilever spring. After calibration the AFM tip was placed in correspondence of a cell in a way that each map covered almost all the cell body. Each acquisition generated a map of force-indentation curves of 30 x 30 micron, divided into 256 pixels (16 on each side), in which each pixel corresponded to a single force-distance curve (Fig 1 b,c). The force-distance curves are recorded at a speed of 2 μm/s. A PNP-DB cantilever (NanoWorld AG) with a pyramid-shape tip and a square base was used to indent the cell surface [11]. The cantilever was made up of silicon nitride Si3N4, with a nominal spring constant of 0.06 N/m and a resonant frequency equal to 17 kHz. The cantilever was coated the back by a thick layer of 70 nm of chromium or gold to increase the reflectance to the laser light.

2.1.5. Force – Distance Curves: Processing and Analysis

Recorded data needed to be postprocessed, prior to the extraction of relevant mechanical parameter. Postprocessing was performed with JPK Data Processing software (JPK Instruments AG) (Fig. 1a).

The first operation consisted in setting the parameters from the previous calibration of the cantilever: sensitivity and spring constant. In this way the raw data in the form of deflection (V)-height (nm) are transformed in force (nN)-height (nm) suitable for subsequent analysis.

In the second step noise of the data was reduced with a Gaussian filter.

The third operation consisted in the subtraction of a baseline to the curve so that the free approach of the cantilever towards the surface was set at zero force. Indeed the cantilever is still in the approach phase to the cell surface. In the case of non-horizontal baselines, a linear tilt to edit the slope of the curve was performed. The contact point is the height of the actuator at which the AFM tip comes into contact with the cell surface.

The fourth step of the force curves post processing concerns contact point determination. This function calculates the point where the force curve crosses the zero force line, and sets this as the zero of the x axis.

Then, we calculated the tip sample-separation. This operation automatically corrects the height signal for the bending of the cantilever to calculate the tip-sample separation. In fact, the height signal that is derived from the piezo displacement contains both, the distance that the cantilever travelled towards the sample and the bending of the cantilever into the opposite direction. For the application of elasticity fits, plots of force against tip-sample separation rather than piezo displacement are needed. With this operation we automatically corrected the signal.

The last operation, called Elasticity fit, automatically applies the Hertz model for the calculation of Young's modulus within defined tip-sample separation intervals. The upper limit was kept constant at 200 nm, whereas the lower boundary was gradually varied from 100nm down to 500nm. This was done in order to assess variations in the extrapolated modulus as a function of the indentation depth. The tip shape employed in the experiment was the square-based pyramid. The Hertzian model was modified by means of the Bilodeau relation:

$$F = 0.7453 \frac{E}{1 - v^2} \delta^2 \tan \alpha$$

where F is the force, E is the Young Modulus, ν is the Poisson's ratio, δ is the indentation value and α represents the opening angle of the pyramid.

Processing of each curve generates two values: Young's modulus and contact point value. Through the latter it's possible to calculate the true height, that is the real height of the cell referred to by the contact point. The true height is calculated by subtracting the average value of substrate contact point from the value of contact point of each cell. Higher values of true height are located at the nuclear region, whereas the lowest values correspond to the lamellipodia. To characterize the cell mechanics, we have identified two areas of interest: the nuclear and cytoplasmic region (Fig. 2). After sorting the Young's modulus according to increasing values of true height, the mechanical properties of the nuclear region were defined by taking the upper 5% of the total values of the elastic moduli with the higher true height. For the mechanical properties of the cytoplasmic region, first of all has been identified the midpoint of the cell height, and then it is taken 5% of the modules above and below the midpoint value.
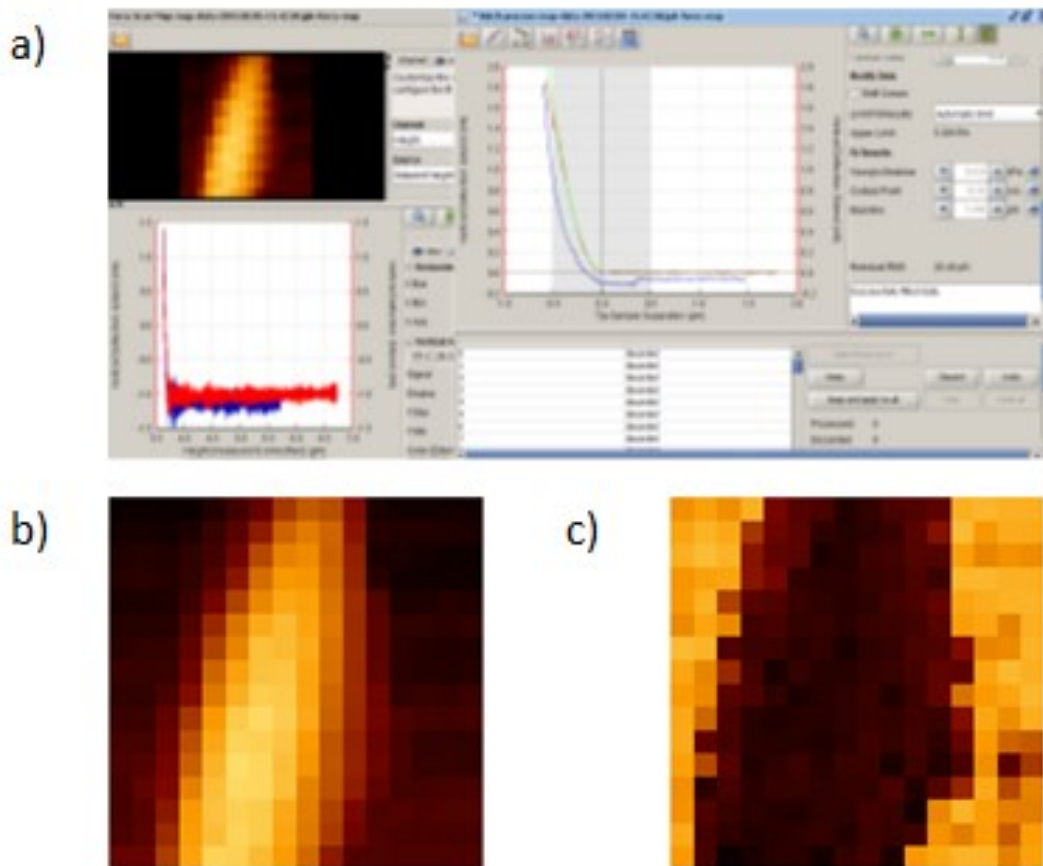
Fig. 1 a) Image of JPK Data Processing, the software used to processing the force distance curves, b) the map of cell height and c) slope map detected with AFM.
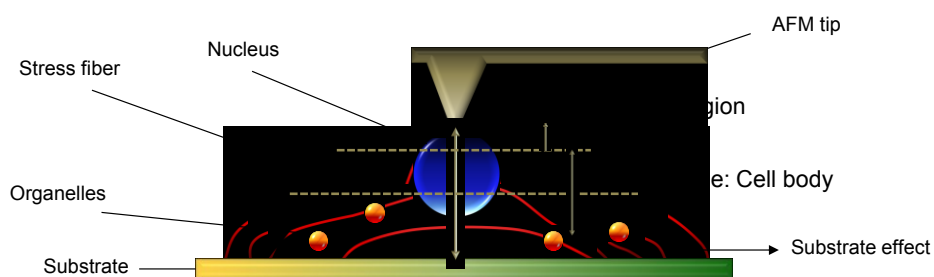
Fig. 2 Representative image of the two regions of interest chosen for the mechanical characterization: nuclear region and cytoplasmic area.

2.1.6. Immunofluorescence Assay

Cells were fixed in paraformaldehyde 4% (w/v) (Sigma) for 20 minutes at room temperature, then samples were washed in PBS and the cell membrane was permeabilized with 0.1% Triton X-100 (Sigma) in PBS. A washing in PBS was then performed and samples were incubated with the nuclear dye Sytox Green (1:1000, ThermoFisher) for 15 min at 37°C. After incubation, the substrates were washed in PBS and actin filaments were stained with TRITC-conjugated phalloidin (1:200, Sigma) for 30 min at RT.

2.2. RESULTS AND DISCUSSION

2.2.1. Correlation Of Modulus-Indentation

In order to obtain a modulus-indentation correlation in all samples, we calculated the averages of Young's moduli of both nuclear and cytoplasmic regions obtained in correspondence of 100 nm indentation and we plotted these values against the averages of the Young's moduli that determined with indentation values of 200 nm, 400 nm and 500 nm. (Fig. 3-10).

We can observe, that the means of the elastic moduli for each correlation are scattered around different lines, whose angular coefficients are around unit value. Indeed, it can be inferred that the cell surface is not a linear elastic material, since, otherwise, the different points would collapse on the quadrant bisector.

As expected we found a better fitting (higher R^2 values) in case of the correlation of moduli evaluated at 200nm against those evaluated at 100nm. Yet, the extent of scattering suggest that both nuclei and cytoplasm are non-linear, in which case we should have found an indentation independent modulus and also heterogeneous. In

particular the cytoplasm appears to be highly heterogeneous owing to the consistently low R^2 values. The analysis of nuclear and cytoplasmic region moduli revealed broad heterogeneities in the distribution of moduli. The sources of these heterogeneities are various: intrinsic biological variability; experimental noise; inaccurate data fitting.
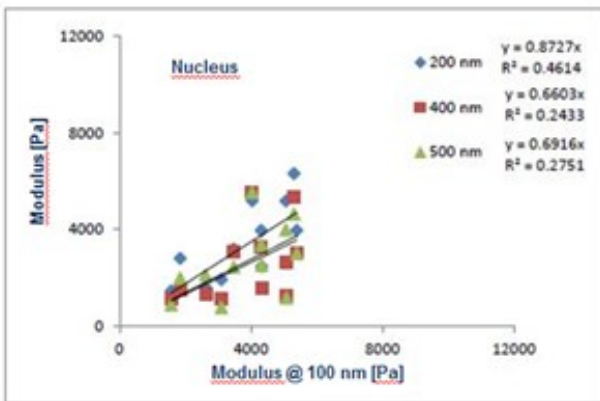
Fig. 3 Correlation graph sample hMsc
Pt FN 700nm (nuclear region)
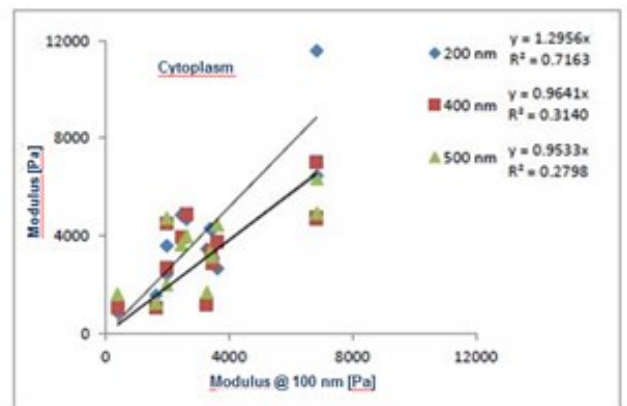
Fig. 4 Correlation graph sample hMsc
Pt FN 700nm (cytoplasmic area)
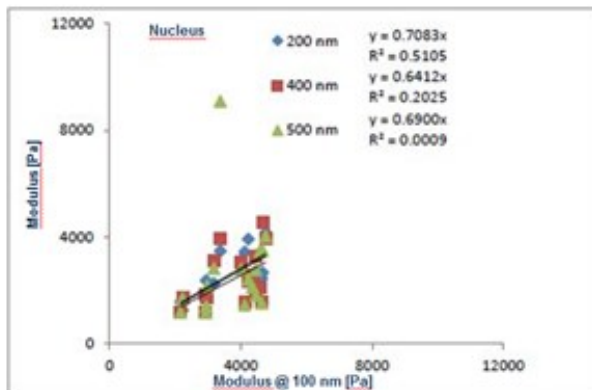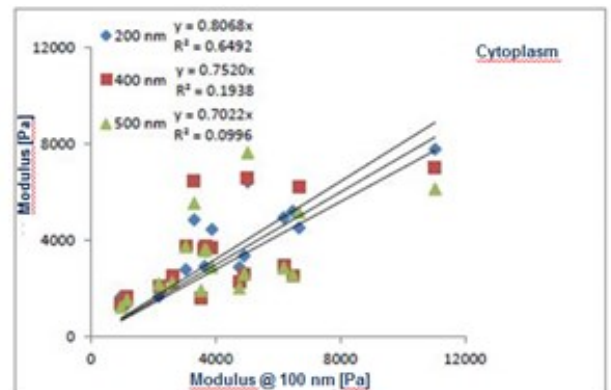
Fig. 5 Correlation graph sample hMsc
Pt FN FLAT (nuclear region)

Fig. 6 Correlation graph sample hMsc
Pt FN FLAT (cytoplasmic area)
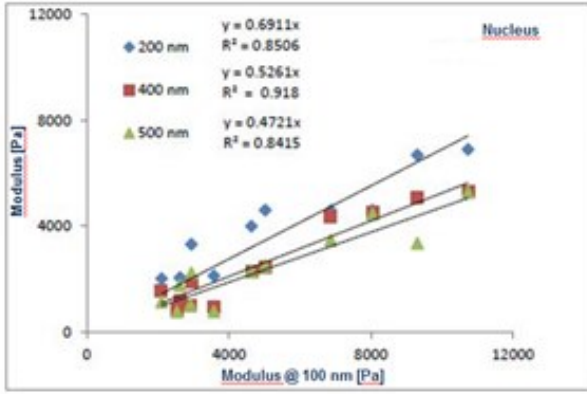
Fig. 5 Correlation graph sample hMsc Pt FN FLAT (nuclear region)
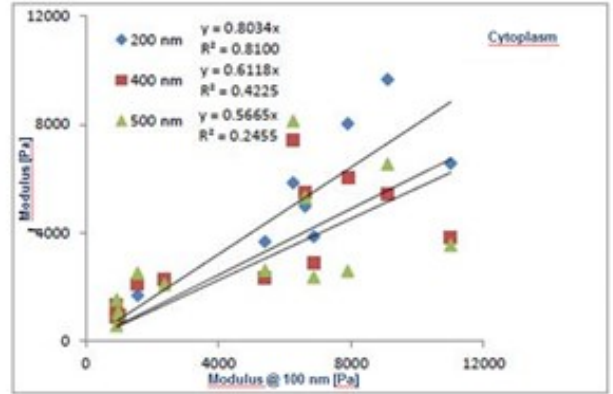
Fig. 6 Correlation graph sample hMsc Pt FN FLAT (cytoplasmic area)
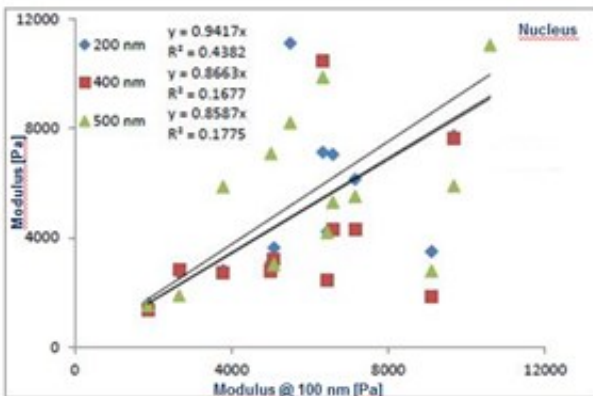
Fig. 7 Correlation graph sample hMsc Pt FBS 700nm (nuclear region)
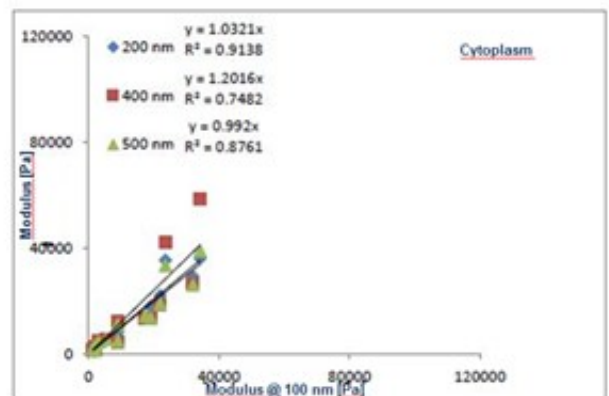
Fig. 8 Correlation graph sample hMsc Pt FBS 700nm (cytoplasmic area)

2.2.2. Statistical Analysis and Outliers Detection

In fact, we found values ranging from few *Pa* up to hundreds of *MPa,* which are clearly non-physiological values.

This might cause problems when comparing different data-set, in which possible relevant differences are masked by the enormous heterogeneity. An important step in the reduction of the variance of the distribution is the outlier removal. This process must be operator independent, robust and consistent. To develop a procedure with these characteristics we observed that the different distributions of Young's moduli are characterized by a log-normal trend, i.e. they are probability distributions of random variables whose logarithm follows a normal distribution. Exploiting this property, outliers can be detected from probability plots. This chart allows you to quickly see if the distribution is really log normal and allows you to check the values range of elastic modulus for which this condition is satisfied. Usually, it was observed that in the range between 10° and 90° percentile the distribution is log-normal. Therefore, all data outside of this interval were not considered for the determination of the summary values.

The probability density plots (Fig. 11, the other plots are shown in the Appendix A) were determined using the calculation program MATLAB. The graphs were obtained for all the samples and for each level of indentation. Moreover, for each specimen there is a graph relating to the nuclear area and one relative to the cell body. The outliers are shown in red ovals.
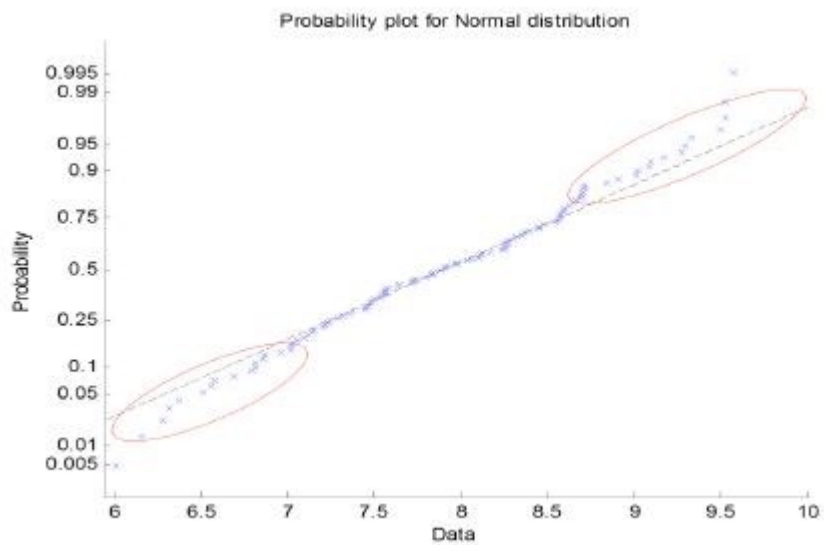
Fig. 11 Representative probability Plot 100nm nuclear region hMsc 700nm Pt FN. Other plots are shown in the Appendix A.

2.2.3. Comparison of the Young's moduli- penetration depths in the different experimental conditions

After the removal of outlier from the moduli distribution, we plotted the average values (± s.e.m.) of the moduli at different indentation depths in the form of histograms (Fig. 12-15). In all the samples tested, the average modulus of the nuclear region displays a decreasing trend with increasing penetration depth of indenter. Similar results were observed for the moduli of the cytoplasmic region of cells cultivated on flat surfaces. Conversely cells seeded on 700 nm nanopatterned substrates display cytoplasm whose moduli do not follow a specific trend. Such characteristic trends suggest a very different mechanical behavior of the nuclear and cytoplasmic region. In more details, the nuclear region appears to be isotropic with an elasto-plastic behavior, by which deeper penetration probe a "softer" material. Similar behavior is observed in cytoplasmic regions of cells cultured on flat

substrates which suggest that the randomly oriented actin network, along with the cytoplasmic substance endows the cytoplasm with elastoplastic mechanical properties. Conversely, when seeded on nanopatterned surfaces, actin filaments form arrays of thick parallel bundle. It is therefore reasonable to assume that the heterogeneity and scattering observed in the cytoplasm region moduli arise from the peculiar assembly of actin bundles.
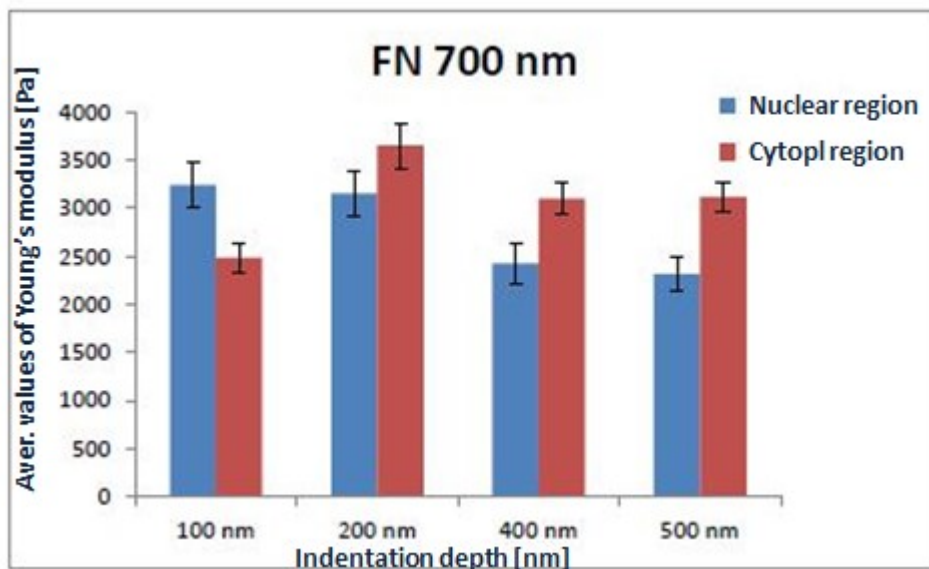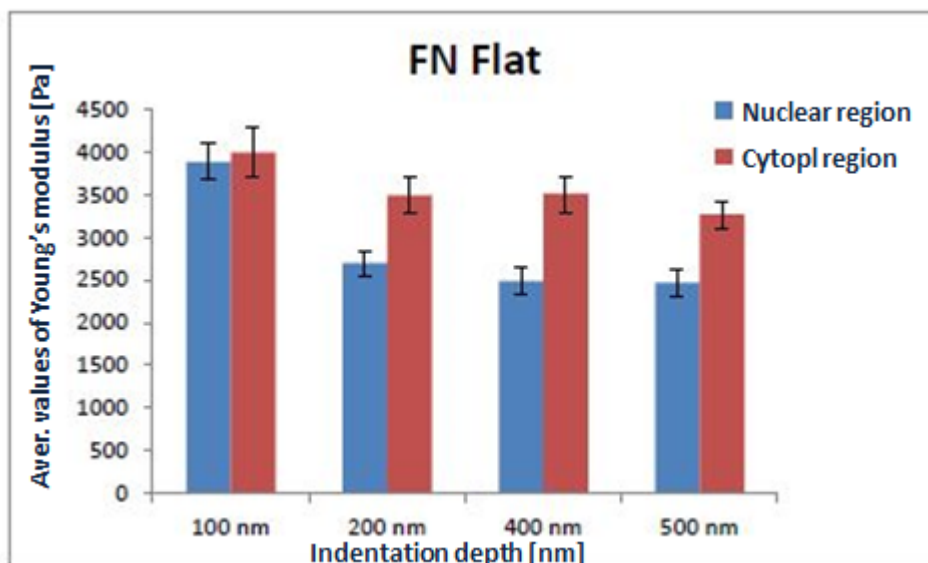

Fig. 12 Bar-chart sample hMsc Pt FN 700nm nuclear and cytoplasmic area.

Fig. 13 Bar-chart sample hMsc Pt FN FLAT nuclear and cytoplasmic area
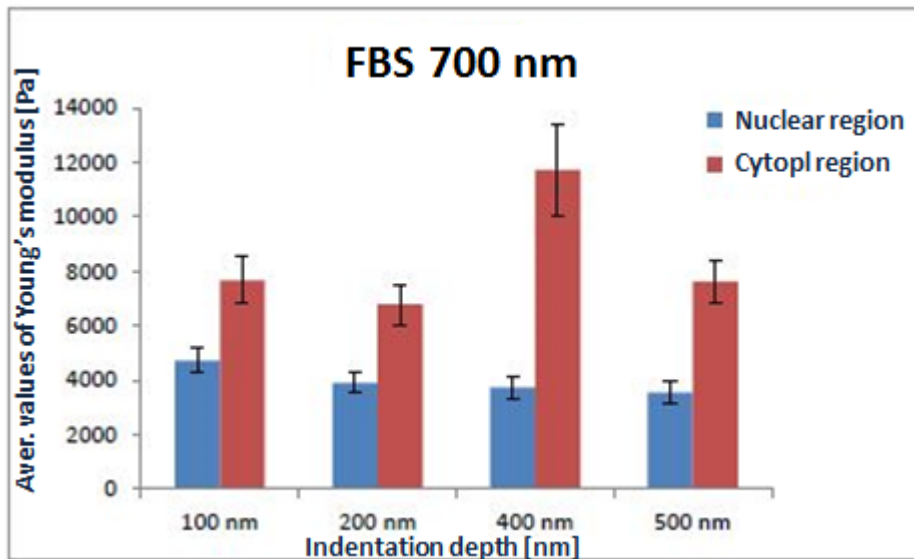
Fig. 14 Bar-chart sample hMsc Pt FBS 700nm nuclear and cytoplasmic area.
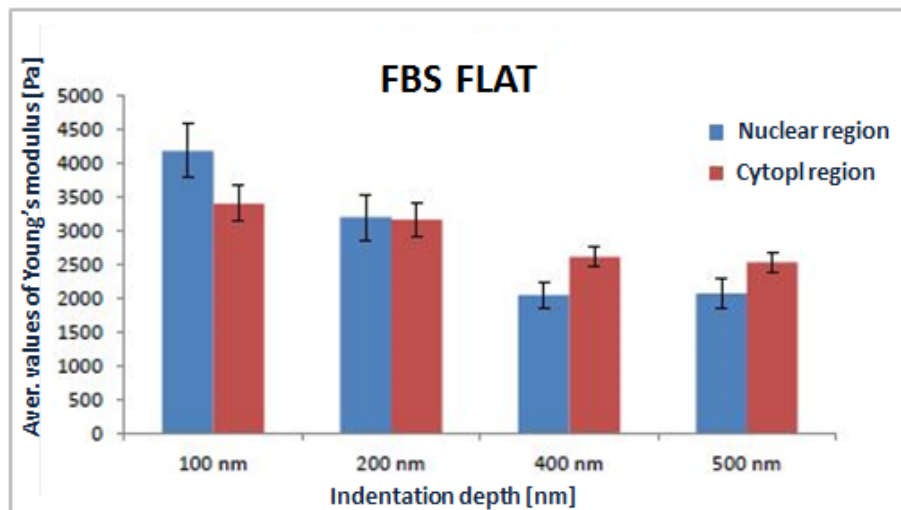
Fig. 15 Bar-chart sample hMsc Pt FBS FLAT nuclear and cytoplasmic area.

In order to correlate the observed heterogeneities of the cell mechanical properties with the morphometric features of the cells in the different experimental conditions, immunofluorescence investigations of the actin cytoskeleton and the nuclear region were carried out.

2.2.4. Morphological investigation

Confocal microscopy observations revealed cells with dramatic morphological differences. In details, stem cells seeded on 700nm nanopatterned substrates and incubated with serum-supplemented culture medium, referred to FBS (Fig. 16a), showed a well-organized cytoskeletal network, actin fibers were aligned along the pattern direction and the peripheral actin bundles flanked the nucleus. Instead, cells cultivated on 700nm patterned materials incubated with fibronectin solution, referred to FN (Fig. 16c), also displayed an actin cytoskeleton aligned along the nanopattern direction, but not all the fibers wrapped the nucleus around: several stress fibers were found far from the nucleus. As regards cells on flat surfaces (Fig. 16b,d), we observed a non-organized actin network, non-oriented stress fibers and a disengaged nucleus from actin fibers. We hypothesized that these morphological heterogeneities were due to the combined effect of nanotopography and different surface treatments.
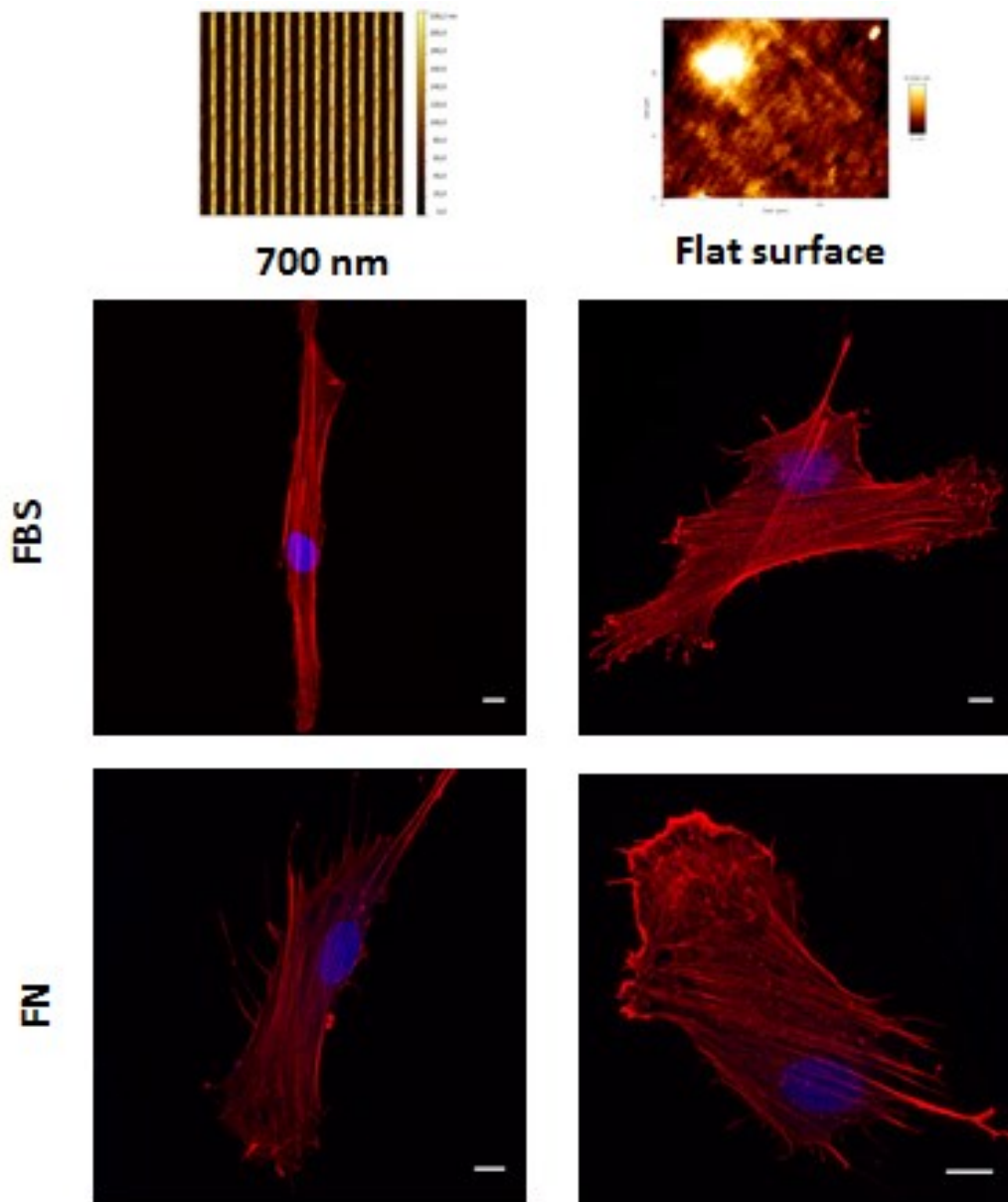
Fig. 16 Confocal microscopy images of hMsc seeded on (a,c) 700nm nanopatterned substrates and (b,d) flat surface. Actin fibers were stained with TRITC-phalloidin (red) and nuclei were stained with sytox green (blue). Scale bars are 10 μm.

In conclusion, cell modulus is both position and indentation dependent, which means that the cell is heterogeneous and not linearly elastic. Assuming that the Hertz model can still used, by changing indentation depth different intracellular structures could be probed. In particular, nuclear region modulus is high for low penetration depth (100-200 nm). This is probably caused by the presence of the cell

cortex, the cytoskeleton and the membrane, and the presence of the nuclear envelope, which are particularly stiff. Conversely, by increasing the indentation value (400-500 nm), mechanical property of the nucleus reflects also the stiffness of the chromatine, since the probe has largely deformed the nuclear envelope. As regards the cytoplasmic area, it is a completely heterogeneous material and for this reason is not felt a specific trend for the elastic modules.

References

1. Swift J, Discher DE. 2014. The nuclear lamina is mechano-responsive to ECM elasticity in mature tissue. J. Cell Sci. 127:3005–15

2. Isermann P, Lammerding J. 2013. Nuclear mechanics and mechanotransduction in health and disease. Curr. Biol. 23:R1113–21

3. Swift J, Ivanovska IL, Buxboim A, Harada T, Dingal P, Pinter J, Pajerowski JD, Spinler K, Shin J, Tewari M, Rehfeldt F, Speicher D, Discher DE. 2013. Nuclear Lamin-A Scales with Tissue Stiffness and Enhances Matrix-Directed Differentiation. Science 341, 1240104

4. Moeendarbary E, Harris AR. 2014. Cell mechanics: principles, practices, and prospects. Syst Biol Med. 6:371–388

5. Crocker JC, Hoffman BD. 2007. Multiple Particle Tracking and Two-Point Microrheology in Cells. Methods in Cell Biology. doi:10.1016/S0091-679X(07)83007-X

6. Neuman KC, Nagy A. 2008. Single-molecule force spectroscopy: optical tweezers, magnetic tweezers and atomic force microscopy. Nat Methods. 5(6): 491–505.

7. Liu H, Wen J, Xiao Y,Liu J, Hopyan S, Radisic M, Simmons CA, Sun Y. 2014. In Situ Mechanical Characterization of the Cell Nucleus by Atomic Force Microscopy. ACS Nano. doi:10.1021/nn500553z

8. Haase K, Pelling AE. 2015. Investigating cell mechanics with atomic force microscopy. J. R. Soc. Interface 12: 20140970. http://dx.doi.org/10.1098/rsif.2014.0970

9. Kasas S, Longo G, and Dietler G. 2013 Mechanical properties of biological specimens explored by atomic force microscopy. Journal of Physics. doi:10.1088/0022-3727/46/13/133001

10. Radmacher M. 2002. Measuring the Elastic Properties of Living Cells by the Atomic Force Microscope. Method in Cell Biology. Vol 68 pp 67-90.

11. Rico F, Roca-Cusachs P, Gavara N, Farre R, Rotger M, Navajas D. 2005 Probing mechanical properties of living cells by atomic force microscopy with blunted pyramidal cantilever tips. Phys. Rev. E 72, 021914.

CHAPTER 3

EFFECTS OF NANOPATTERNING ON CELL AND NUCLEAR MORPHOLOGY AND MECHANICS

Mechanotrasduction focuses on how cells convert mechanical forces into gene expression [1]. All multicellular organisms are subject to a multitude of forces arising from the neighboring environment, such as compressive forces or shear forces and the balance of them is critical to the development and maintenance of tissue. The way in which cells respond to these stresses is strongly dictated by the intrinsic cell mechanics, by cell-cell contacts and from the extracellular matrix (ECM), indeed most of the biophysical extracellular signals derive exactly from ECM [2]. These mechanical cues influence different aspects of cell behavior such as adhesion, proliferation, migration and differentiation. In this context, through the adhesion processes, these kinds of signals interfere with the dynamics of focal adhesions (eg. Talin, vinculin) development, which are great proteic complexes that, through the cellular cytoskeleton, are connected to the extracellular matrix [3]. Even the cytoskeleton, skeletal support of the cell, is affected by the mechanical stimuli that arrive from the neighboring environment. In a recent study stem cells seeded onto stiff substrates were shown to exhibit contractile phenotype and well-developed focal adhesions. On the other hand, cells seeded on soft substrates display an immature cytoskeleton and unstable focal adhesions. By a biochemical point of view, these results lead to the activation of stress-dependent pathway (eg. FAK phosphorylation) and nuclear membrane deformation [4]. Therefore, the same biophysical signals expressed by the biological material, the extracellular matrix, may be displayed by a non-biological material, or rather a suitably instructive material able to activate the same mechanisms of mechanotransduction into the cells [5]. However, little is known about how material cues can produce a specific

assembly of the cytoskeleton and alter the cell mechanics. In this chapter we show how, by using nanotopographic patterns, we were able to induce a characteristic cytoskeletal arrangement and typical intracellular stress state. For this purpose two different substrates were used, namely: 700nm and 350nm patterned materials. These were functionalized with two surface treatments in order to modulate two aspects. These two substrates allows to control FA growth and orientation, which in turn affect cytoskeleton assembly and contractility.

3.1. MATERIALS AND METHODS

3.1.1. Fabrication of Nanopatterned Substrates

Nanopatterned substrates were fabricated by replica molding of polydimethylsiloxane (PDMS, Sylgard184- Dow Corning) on a polycarbonate master. Two types of masters were used: one with 700nm wide ridges, 700nm wide grooves and a groove depth of 250 nm, the other with 350nm wide ridges, 350nm wide grooves, and a groove depth of 100 nm. PDMS was prepared by mixing elastomer base and curing agent at a 10:1 weight ratio. PDMS solution was degassed, poured onto the polycarbonate master and then cured at 37 °C for 24 h. Control flat substrates were produced by pouring the base and curing mix on a 35 mm polystyrene Petri dish (Corning) and curing at 37 °C for 24 h.

3.1.2. Functionalization of Substrates

Substrate adhesivity was altered through two types of functionalization. All PDMS samples were treated with oxygen plasma for 1 min and then incubated with serum-supplemented culture medium (10%) at 37 °C (samples referred to as FBS) or

fibronectin (Fibronectin from Human Plasma, Sigma) solution (10 µg/ml) at 4 °C (samples referred to as FN) overnight prior to cell seeding.

3.1.3. Cell Culture

Human Mesenchymal Stem Cells (hMSCs) were purchased from Lonza and cultured in α-MEM (Modified Eagle's Medium, Bio Whittaker) supplemented with 10% fetal bovine serum (FBS, Euroclone), 100 mg/ml L-glutamine, 100 U/ml penicillin/streptomycin (Sigma). Cells were cultured on functionalized surfaces and incubated in a humidified atmosphere at 37 °C and 5% CO_2 for 48h.

3.1.4. Immunofluorescence Assay

Immunofluorescence staining was carried out according to the following procedure. Cells were fixed in paraformaldehyde 4% (w/v) (Sigma) for 20 minutes at room temperature, then samples were washed in PBS and the cell membrane was permeabilized with 0.1% Triton X-100 (Sigma) in PBS. Then, to avoid non-specific binding, the samples were incubated with a solution of PBS / 1% BSA for 30 minutes. To identify the focal adhesions, the samples were incubated with an antivinculin monoclonal antibody (1: 200, Millipore) and allowed to incubate for 2 h in an humid chamber. Afterwards, the substrates were washed three times in PBS/BSA 1% and then incubated with a secondary antibody, Alexa Fluor 647 conjugated goat anti-mouse (1: 300, ThermoFisher) while actin filaments were stained with TRITC-conjugated phalloidin (1:200, Sigma) for 30 min at RT. After incubation, three washes were performed in PBS and the samples were incubated with the nuclear dye Sytox Green (1: 1000) for 15 min at 37 ° C. Samples were left in the saline buffer until the observation through confocal microscopy. In a level up experiment to

detect lamins A/C has been used a goat polyclonal antibody (1:200, Santa Cruz Biotecnology) and then an Alexa Fluor 488 donkey anti-goat (1:300, ThermoFisher). In a further staining in addition to the actin fibers, stained as previously indicated, samples were incubated with the nuclear dye DAPI (1: 1000, Invitrogen) for 5 min at 37 ° C for the evaluation of nuclear features.

3.1.5. AFM Experiment

A JPK NanoWizard II AFM (JPK Instrument) was used to measure mechanical properties of living cells. An optical microscope was combined with the AFM to position AFM tips on a particular sample location. Soft cantilevers (PNP-DB, nominal spring constant 0.06 N/m, NanoWorld AG) were used to investigate cell mechanical properties. The force-distance curves were acquired in contact mode. Prior to acquisition, the spring constant of each cantilever was first calibrated by the thermal noise method. Each acquisition generated a map of force-indentation curves of 30 x 30 micron, divided into 256 pixels (16 on each side), wherein each pixel corresponded to a force-distance curve. The force-distance curves were recorded at a speed of 2 μm/s. After indentation, each force-distance curve was processed using the software JPK Data Processing (JPK Instruments AG) and the Hertzian model was used to calculate Young's modulus for every force curve.

3.1.6. Morphometric Analysis

Cell and FA morphometry measurements were performed by using Fiji software. Morphometric analysis of focal adhesions was performed as follows. Digital images of FAs were firstly processed using blur command by following a modified procedure of the one proposed by Maruoka et al [6]. Blurred image were then subtracted from

the original images using the image calculator command. The images were further processed with threshold command to obtain binarized images. Pixel noise was erased using the erode command and then particles analysis was performed in order to extract the morphometric descriptors. Morphometric data were analyzed with Matlab. Statistical significance was assessed by means of a non-parametric Kruskale-Wallis test.

Cell polarization was assessed from TRITC-phalloidin stained cells that were analyzed with the MomentMacroJ v1.3 script (hopkinsmedicine.org/fae/mmacro.htm) run in Fiji. Briefly, the macro calculates the second moment of grey scale images. For our purposes, we evaluated the principal moments of inertia (i.e. maximum and minimum) and the cell polarization was defined as the ratio of the principal moments (max/min).

3.2. RESULTS AND DISCUSSION

3.2.1. Morphological Characterization OF Cells and Focal Adhesions

Immunofluorescence staining were performed in order to gain information on cell and FA morphology, along with cytoskeleton assembly. Confocal examination of stained samples revealed strong morphological heterogeneities of the cell body (Fig.1).
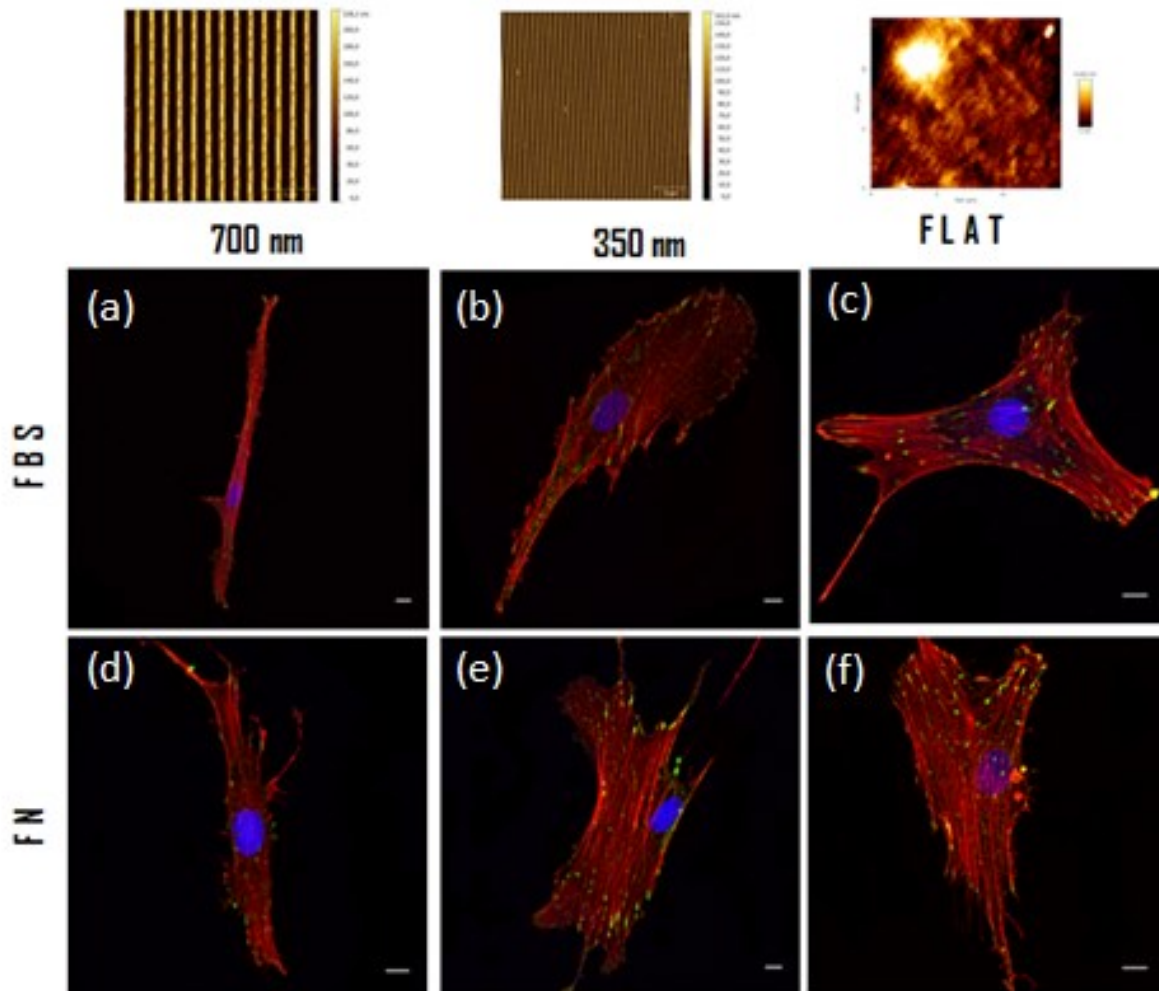
Fig. 1 Confocal microscopy images of hMsc cultivated on (a,d) 700nm nanopatterned substrates, (b,e) 350nm pattern and (c,f) flat surface. Actin fibers were stained with TRITC-phalloidin (red), FAs immunostained for vinculin (green) and nuclei were stained with sytox green (blue). Scale bars are 10 μm.

In details, hMsc cultivated on 700nm nanopatterned substrates and incubated with serum-supplemented culture medium, referred to FBS (Fig. 1a), exhibited a distinctly spindle-like phenotype, stress fibers were aligned along the pattern direction and in close contact with the nucleus. On 700nm nanograting surfaces incubated with fibronectin solution, referred to FN (Fig. 1d), cells showed actin bundles that follow the topography but, in this case, we observed a smaller number of stress fibers that

are close to the nuclear envelope. Instead, as regards cells seeded on 350nm pattern display a well arranged cytoskeleton and, also in this case, on FBS treated materials (Fig. 1b) cells exhibit stress fibers near the nucleus, meanwhile on FN treated surfaces (Fig. 1e) a higher number of actin fibers is located farther from the nucleus. On the control flat surfaces (Fig. 1c,f), stem cells develop a randomly organized cytoskeleton, actin bundles extended in all directions and the nucleus appeared to be disengaged from stress fibers. We have attributed these marked morphological differences to the combined presence of patterned surfaces and different adhesion treatment. Our hypothesis is that, through the adhesiveness linked to the nanotopography, it is possible to control the growth of focal adhesion in terms of size; therefore, to verify this hypothesis, we performed an analysis on FA length on nanopatterned surfaces and flat substrates. The results of this analysis showed that the FA length of cells cultured on 350nm pattern was always lower than FAs grow on 700nm nanopattern (Fig.2). This data demonstrated that the type of surface functionalization we chose was effective in controlling FA features, promoting the development of longer FAs on 700nm substrates.
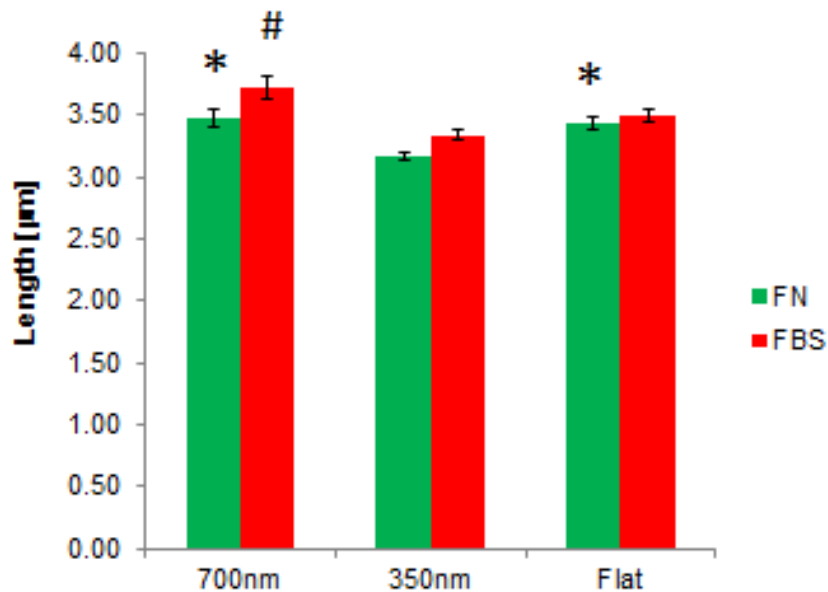
Fig. 2 Histogram of focal adhesion length (Feret's length) measured on nanopatterned substrates (700nm and 350nm) and flat surface, incubated with serum-supplemented culture medium (red) or fibronectin solution (green). Error bars are s.e.m. *,# indicate significant difference w.r.t. 350 nm.

Thus, these data along with the morphological observations suggest that the nanopatterning and biochemical functionalization alter FA shape which impact stress fiber assembly and contractility. Since stress fibers might be directly connected to the nuclear envelope and might transfer on this compressive forces, it is likely that stress fibers can deform the nucleus through myosin contraction. This might be particularly evident in case of parallel arrays of actin bundles which exert a coordinated action on the nucleus, which occurs on nanopatterned substrates. Then we investigated whether a correlation between nuclear aspect ratio (A/R) and cell polarization existed (Fig.3). Analyzing the case of cells seeded on 700 nm FBS and 350 nm FBS patterned surfaces, these are highly polarized and with a high nuclear A/R and therefore with a very spindle-like morphology. This process occurs because the longitudinal FAs are more stable than transversal FAs as longitudinal ones have

39

greater chance to grow along the direction of the pattern, unlike transverse FAs that promote the lateral cell collapse with the consequent fusiform phenotype.

On nanopatterned materials incubated with fibronectin solution (10μg/mL), we observed a low degree of polarization on 350nm FN surfaces. This event is caused by the presence of fibronectin which retains the transversal FA and impedes the polarization. Instead in the case of 700nm FN, FAs can grow better along the direction of the pattern, an increased cell contractility is promoted and cell with its actin network tends to develop along the pattern direction.

As regards control flat surfaces we can read for all samples a low degree of polarization and a low nuclear A/R because FAs, in this case, are in no way confined in the growth and orientation, it is arranged randomly and consequently the stress fibers and the cytoskeleton do not exert any compressive force over the nucleus.

Thus even through FN coated substrates promote well defined and visible stress fibers assembly, these can also be stabilized on the cell periphery. Thus they do not exert any stress on the nucleus. Conversely, cells on FBS coated substrates possess the majority of stress fibers on the nucleus which more effectively compress it despite the reduced formation of FA.
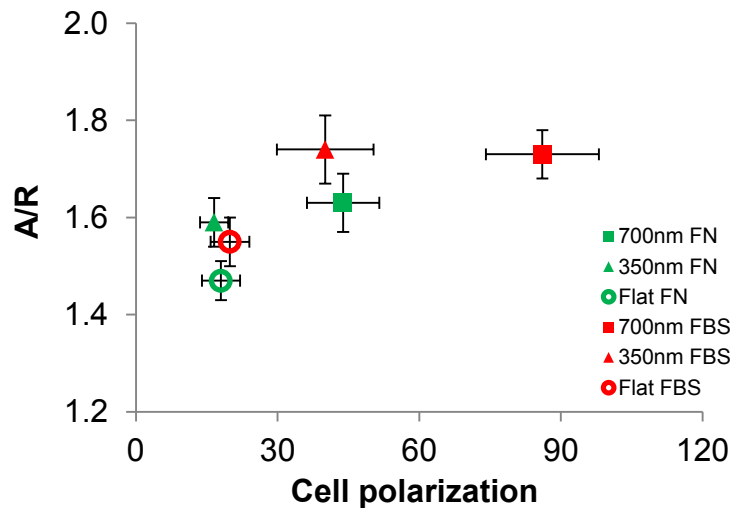
Fig. 3 Scatter plot that correlates nuclear A/R with cell polarization. Error bars are s.e.m.

3.2.2. Mechanical characterization

To better understand the cells behavior on our engineered substrates a mechanical characterization of nuclear and cytoplasmic region, by AFM experiments, was carried out (Fig.4). Cells seeded on flat surfaces displayed a non-organized cytoskeleton to control the nuclear shape, so we recorded low mechanical properties in the nuclear and cytoplasmic region. Instead, on nanograted materials we measured higher cellular mechanical properties, in terms of Young's modulus, index of a greater intracellular stress state. Among the cells cultivated on nanopatterned substrates, those seeded on 350 nm FN pattern have a low cytoplasmic modulus, this suggest a stress state of modest contractility, indeed these cells show a low polarization index and stress fibers are not very effective in the nuclear squeezing. With regards to 350nm FBS pattern, this show a moderately low Young's modulus in nuclear and cytoplasmic region. On this type of topography despite the cells are well polarized and have a high A/R, the contractility is not capable of affect an increase of the mechanical properties. The contractility of this nanotopography is inhibited by the inability of FAs to grow sideways along the

41

direction of the pattern and this does not allow the stress fibers to develop in such a way to create a contractile network.

On the other hand, on 700nm nanograted surfaces the longitudinal FAs have the chance to grow along the pattern and in the case of 700 nm FN also the transverse FA are stabilized by the fibronectin coating that promotes the adhesion stabilizing a population of stress fibers which remains far away from the nucleus without exerting compressive forces on it. Here we recorded higher mechanical properties of the nuclear and cytoplasmic region than 350nm patterned material, because although there is a lower polarization index, there is an increase in contractility attributed to stress fibers that are located around the nucleus.

Cells seeded on 700nm FBS substrates show high mechanical properties in the cytoplasmic area and a high degree of polarization, because thanks to the topography, the longitudinal FA have space to grow and sustain the loads giving rise to stable stress fibers meanwhile transverse FA disassemble leading to lateral collapse of the fibers that you can read in high cell polarization. Conversely, cells on flat surfaces showed a cytoplasm with similar mechanical properties to 350nm nanopatterned materials but totally useless in squeezing the nucleus.
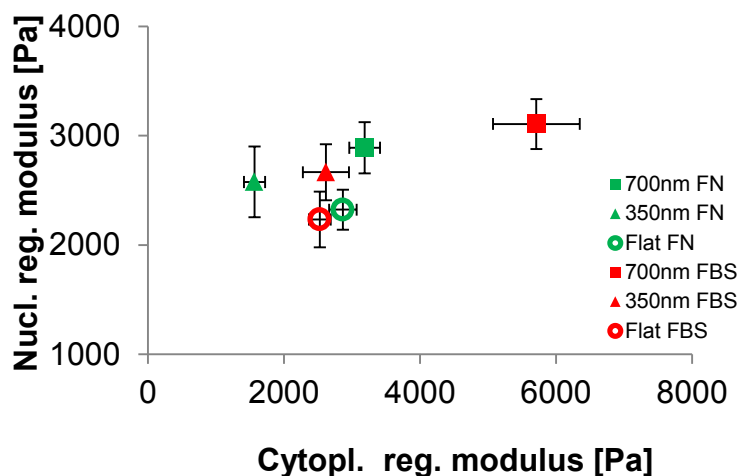
Fig. 4 Scatter plot of nuclear mechanical properties correlated to mechanical properties of cytoplasmic region. Error bars are s.e.m.

Altogether this data showed that the best features are linked to 700nm FBS nanopatterned surfaces, where there is a combined effect given by the coordinated motion of stress fibers, which squeeze the nucleus, and the nuclear contractility. Ascertained the existence of this tensional state around the nucleus, we investigated how this stress state can alter the nucleus in terms of its volume (Fig.5).
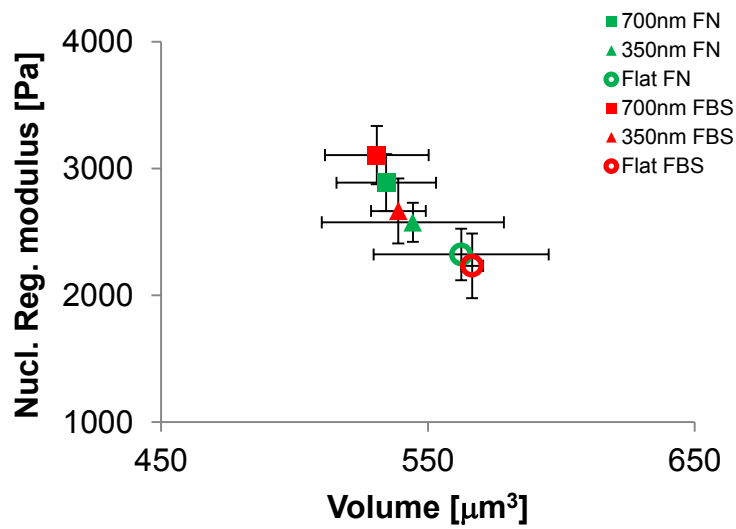
Fig. 5 Scatter plot of nuclear region Young's moduli versus nuclear volume. Error bars are s.e.m.

Here we observe that cells seeded on nanopatterned surfaces recorded high nuclear mechanical properties and low volumes, due to compression forces acting on the nucleus that suggest an higher stress state than flat samples that show greater volumes.

3.2.3. Features that affect nuclear mechanics

The nucleus is a complex organelle, therefore to understand the real structure that dictates nuclear mechanics, we investigated lamins A/C expression (Fig.6). It is

known that lamins play a major role in the maintenance of nuclear shape, stability and structure. Additionally, it is believed that they modulate gene expression [7].
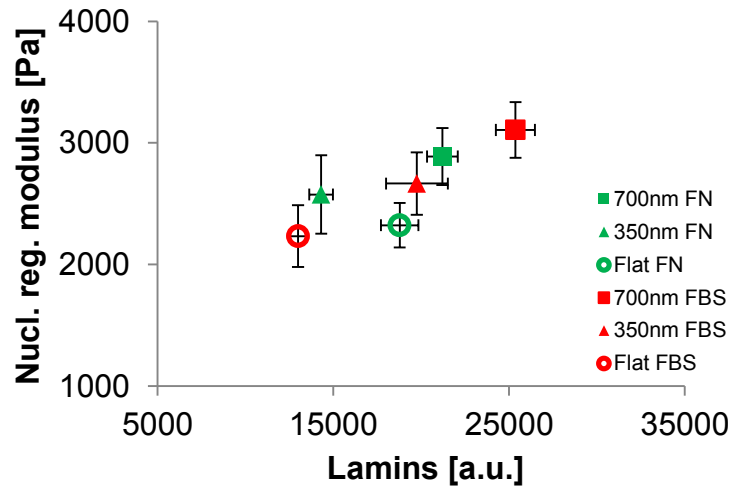
Fig.6 Scatter plot that correlates the mechanical properties in the nuclear region and lamins A/C expression. Error bars are s.e.m.

We can observe a meaningful correlation between the nuclear mechanical properties and lamins A/C expression. Cells on nanopatterned materials revealed high nuclear Young's moduli and an overexpression of lamins A/C. Conversely, flat surfaces showed low mechanical properties and lamins expression. Indeed, the fluorescence intensity increase was due to the presence of a greater stress state inner the cell. These data are consistent with other reports that demonstrate that low intracellular stress states induce the phosphorylation of lamins A/C that leads to their degradation. On the other hand, contractile phenotypes inhibit the phosphorylation of lamins A/C leading to an overexpression [4].

If the volume changes, and there is a good correlation between the nuclear mechanical properties and lamins expression, we asked how the genetic material is reconfigured. To better understand how chromatin densifies, nuclei were stained

with DAPI, that intercalates into minor groove of DNA and z-stacks of confocal images were acquired (Fig.7).
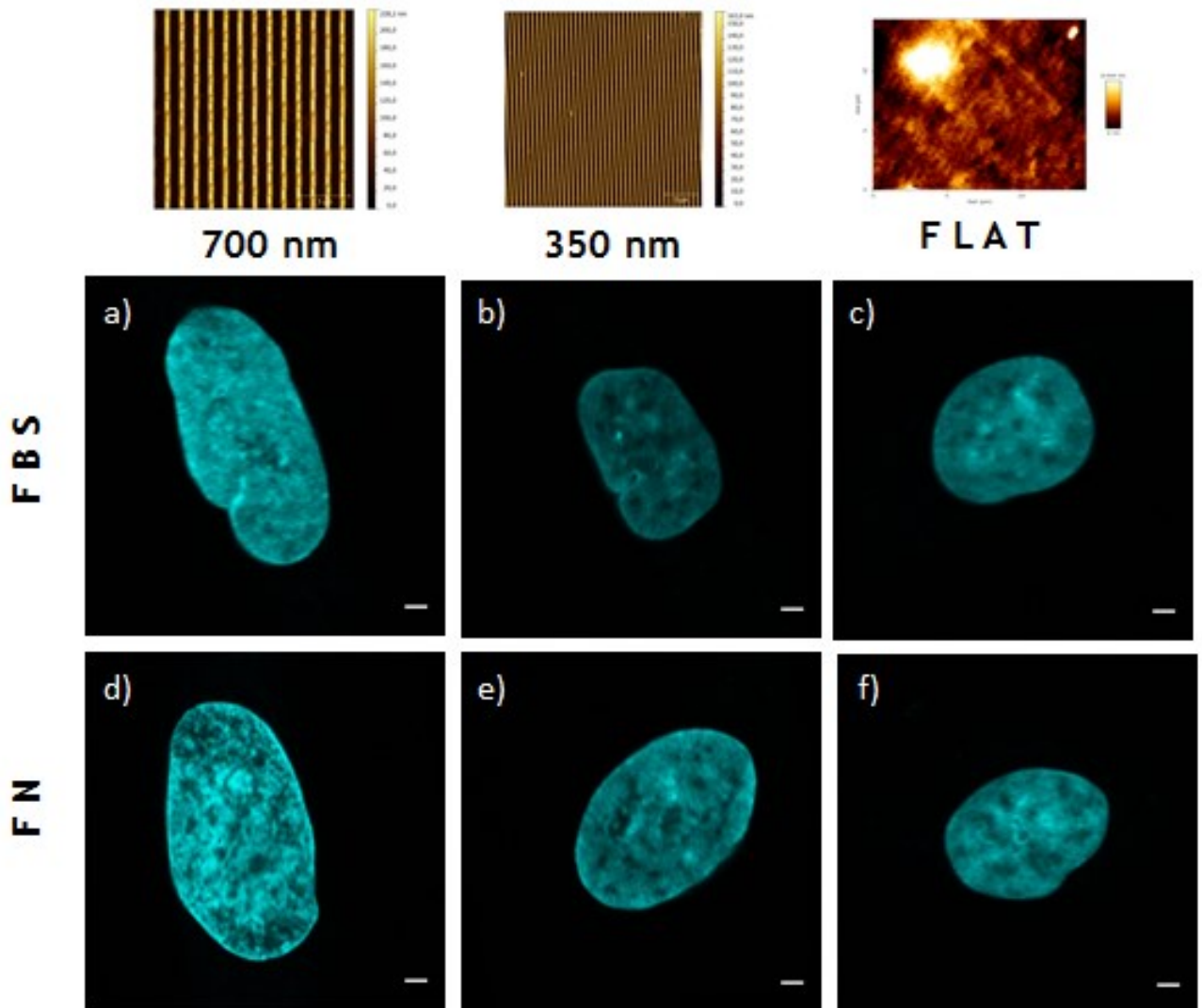
Fig. 7 Confocal images of hMsc nuclei seeded on (a,d) 700nm nanograting substrates, (b,e) 350nm pattern and (c,f) flat surface. Scale bars are 2 μm.

Because the nuclear staining is highly heterogeneous, there are more and less fluorescent areas, we have not integrated all along the z-stack to not miss this heterogeneity information. Conversely, we have assumed the middle slice of the nucleus as a representative of the chromatin densification of the whole nucleus. So, if actin cytoskeleton squeezes the nucleus, and the nucleus has a porous membrane,

we expect a very high intensity fluorescence of nuclear matter for cells that have a very low volume, because the material should be compacted. Instead, cells that have larger volumes should have a lower material density and thus a lower fluorescence intensity.

By results achieved, these assumptions are not verified, indeed cells that recorded intermediate mechanical properties showed low intensity fluorescence of chromatin. Therefore, no significant correlation exists between the nuclear mechanical properties and the genetic material densification (Fig. 8).
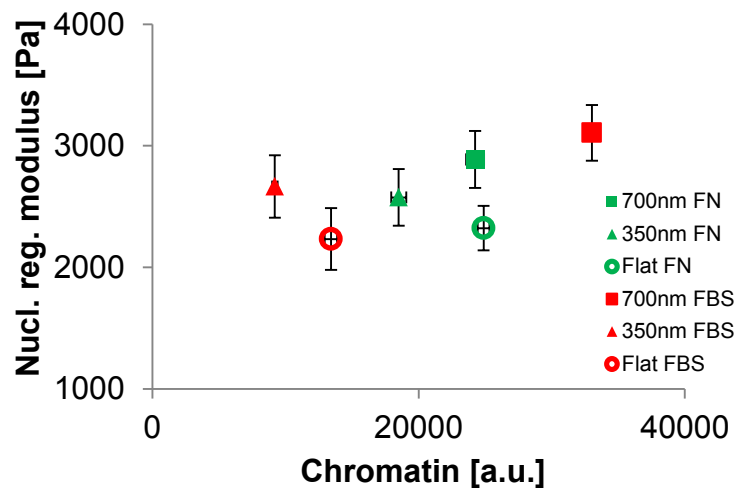
Fig. 8 Scatter plot of correlation of nuclear region modulus and chromatin intensity fluorescence. Error bars are s.e.m.

Overall, this study clearly show that lamins A/C have a primary role in dictating the nuclear mechanical properties, which is in agreement with the role that these proteins have as structural proteins of nucleoskeleton.

References

1. Wozniak MA, Chen CS. 2009. Mechanotransduction in development: a growing role for   contractility. Nature Reviews Molecular Cell Biology. doi:10.1038/nrm2592

2. Chen CS, Tan J and Tien J. 2004 Mechanotransduction at cell-matrix and cell-cell contacts. Annu.Rev. Biomed. Eng. 6, 275–302. doi: 10.1146/annurev.bioeng.6.040803.140040

3. Geiger B, Spatz JP, Bershadsky AD Environmental sensing through focal adhesions. 2009. Nature Reviews Molecular Cell Biology. doi:10.1038/nrm2593

4. Ivanovska IL, Shin JW, Swift J, Discher DE. 2015 Stem cell mechanobiology: diverse lessons from bone marrow. Trends in Cell Biology. doi:10.1016/j.tcb.2015.04.003

5. Ventre M, Netti PA. 2015 Engineering Cell Instructive Materials To Control Cell Fate and Functions through Material Cues and Surface Patterning. ACS Applied materials and interfaces. doi: 10.1021/acsami.5b08658

6. Maruoka M, Sato M, Yuan Y, Ichiba M, Fujii R, Ogawa T, Ishida-Kitagawa N, Takeya T, Watanabe N. 2012. Abl-1-bridged tyrosine phosphorylation of VASP by Abelson kinase impairs association of VASP to focal adhesions and regulates leukaemic cell adhesion. Biochem. J. 441, 889–899. doi:10.1042/BJ20110951.

7. Dahl KN, Ribeiro A, Lammerding J. 2008. Nuclear Shape, Mechanics, and Mechanotransduction. Circulation Research. DOI: 10.1161/CIRCRESAHA.108.173989

CHAPTER 4

EFFECTS OF CELL-CELL CONTACT IN AFFECTING ACTIN CYTOSKELETON ASSEMBLY AND CELL MECHANICS

Cells are continuously subjected to a multitude of signals coming from the surrounding environment. Furthermore, many cell types form large aggregates in vivo, in which extensive cell-cell contact is observed, i.e. epithelia, endothelia. This might be relevant in the context of mechanotransduction in which interactions with neighboring cells affect cell shape and cytoskeleton. Therefore, what is known and occurs at a single level might differ in a cell population set-up. The largest family of proteins that control cell - cell junction is represented by cadherins [1]. The adhesive connections built by these proteins provide mechanical information to cells by withstanding the forces generated by endogenous or exogenous contractile forces. Moreover, cadherin complexes are involved in connection of cytoskeletal network of adjacent cells, and this creates stress state fluctuations. All these mechanisms are placed in mechanotransduction processes and have great relevance in cell differentiation [2]. Along these lines, Liu et al. in 2010 demonstrated that endogenous traction forces on adherent junction in endothelial cells on patterned micropillar triggered an increase in tension across the junction that was produced by actomyosin contractility [3]. Ladoux et al. in 2010 showed that cadherin-mediated mechanotrasductive processes moved through the cellular contractile machinery [4]. Nevertheless, how the intercellular junctions remodeling alters the actin network and the cell mechanics is still little known.

In this chapter we showed how the presence of an extensive cell-cell contact can alter the cytoskeleton architecture and how this eventually affects the nuclear

mechanics. For our purpose, we seeded Human Umbilical Vein Endothelial Cells (HUVEC) on PDMS surface at either sparse or high cell densities. The substrates were functionalized in order to promote cell adhesion on the PDMS. Afterwards, we studied the effect of cell – cell contact, mediated by Ve-Cadherin, on the actin cytoskeletal architecture with high resolution microscopy and then on the intracellular stress state, in terms of mechanical properties, in the cytoplasmic and nuclear region.

4.1. MATERIALS AND METHODS

4.1.1. Surfaces Preparation

Flat substrates were prepared by polymer casting. In particular, a polydimethylsiloxane (PDMS, Sylgard 184 – Dow Corning) solution was prepared. PDMS was prepared by mixing elastomer base and curing agent at a 10:1 weight ratio. PDMS solution was degassed, poured onto a 35 mm polystyrene Petri dish (Corning) and then cured at 37 °C for 24 h.

4.1.2. Functionalization of Substrates

Substrates adhesivity was improved by oxygen plasma treatment for 1 min, then flat surfaces were incubated with a N-Sulfosuccinimidyl-6-(4'-azido-2'nitrophenylamino) hexanoate (Sulfo-SANPAH, Thermo Scientific) solution (0.5 mg/ml in 50 mM HEPES buffer, pH 8.5). PDMS Samples were illuminated with UV light, 365 nm, for 10 min. Then, the excess of solution was removed and the surfaces were exposed to additional 10 min of UV treatment. The substrates, washed twice in PBS, were then

incubated with the fibronectin solution (10 μg/ml in PBS) and stored overnight at 4 °C.

4.1.3. Cell Culture

Human Umbilical Vein Endothelial Cells (HUVEC) were purchased from Gibco and cultured in Medium 200 (Gibco) supplemented with fetal bovine serum (2% v/v), hydrocortisone (1 μg/ml), human epidermal growth factor (10 ng/ml), basic fibroblast growth factor (3 ng/ml), heparin (10 μg/ml) (Gibco). Cells were cultured on treated surfaces at 37°C and 5% CO_2 for 4h and 24h.

4.1.4. Immunofluorescence Assay

Cells were fixed in paraformaldehyde 4% (w/v) (Sigma) for 20 minutes at room temperature, then samples were washed in PBS and the cell membrane was permeabilized with 0.1% Triton X-100 (Sigma) in PBS. After, to avoid non-specific binding, the samples were incubated with a solution of PBS / 1% BSA for 30 minutes. To identify the focal adhesions, the samples were incubated with an antivinculin monoclonal antibody (1:200, Millipore), instead to detect the cadherin an anticadherin monoclonal antibody (1:300, Santa Cruz Biotechnology) was used and allowed to incubate for 2h in a humid chamber. Afterwards, the surfaces were washed three times in PBS and then incubated with a secondary antibody donkey anti goat 546 (1:500, Thermo Scientific) for 45 min. Three washes in PBS were then performed and samples were incubated with a secondary antibody Goat antimouse 647 (1:300, Thermo Scientific). Actin filaments were stained with Alexa Fluor 488 Phalloidin (Thermo Scientific) for 30 min. After 30 minutes three washes were

performed in PBS and the samples were left in the saline buffer before observation with confocal microscopy.

4.1.5. AFM Experiment

A JPK NanoWizard II AFM (JPK Instrument) was used to measure mechanical properties of living cells. An optical microscope was combined with the AFM to position AFM tips on a particular sample location. Soft cantilevers (PNP-DB, nominal spring constant 0.06 N/m, NanoWorld AG) were used to investigate cell mechanical properties. The force-distance curves were acquired in contact mode prior to acquisition, the spring constant of each cantilever was first calibrated by the thermal noise method. Each acquisition generated a map of force-indentation curves of 30 x 30 micron, divided into 256 pixels (16 on each side), wherein each pixel corresponded to a force-distance curve. The force-distance curves were recorded at a speed of 2 µm/s. After indentation, each force-distance curve was processed using the software JPK Data Processing (JPK Instruments AG) and the Hertzian model was used to calculate Young's modulus for every force curve.

4.2. RESULTS AND DISCUSSION

4.2.1. Morphological Characterization

Human Umbilical Vein Endothelial Cells were cultivated on flat substrates for 4h and 24h after seeding at single cell and confluence state. Confocal images showed structural heterogeneity in the assembly of the actin cytoskeleton between single cells and cell populations (Fig. 1,2). Because cadherins are the main proteins that

govern cell-cell adhesion, in the cells seeded at low density on flat surfaces VE-cadherin signal is faint, uniform and mostly cytoplasmic (Fig 1a,d). The surface treatment of the substrates increased cellular adhesion through focal adhesions, which appeared well developed with high-resolution microscopy observations (Fig 1c,f). To better investigate the actin network in single cells and cell populations, z-stacks of confocal images were acquired. In isolated cells, we observed an actin cytoskeleton with stress fibers uniformly distributed in the cytoplasm. These fibers were oriented in the direction of cell polarization and wrapped the nucleus around (Fig 1b,e).
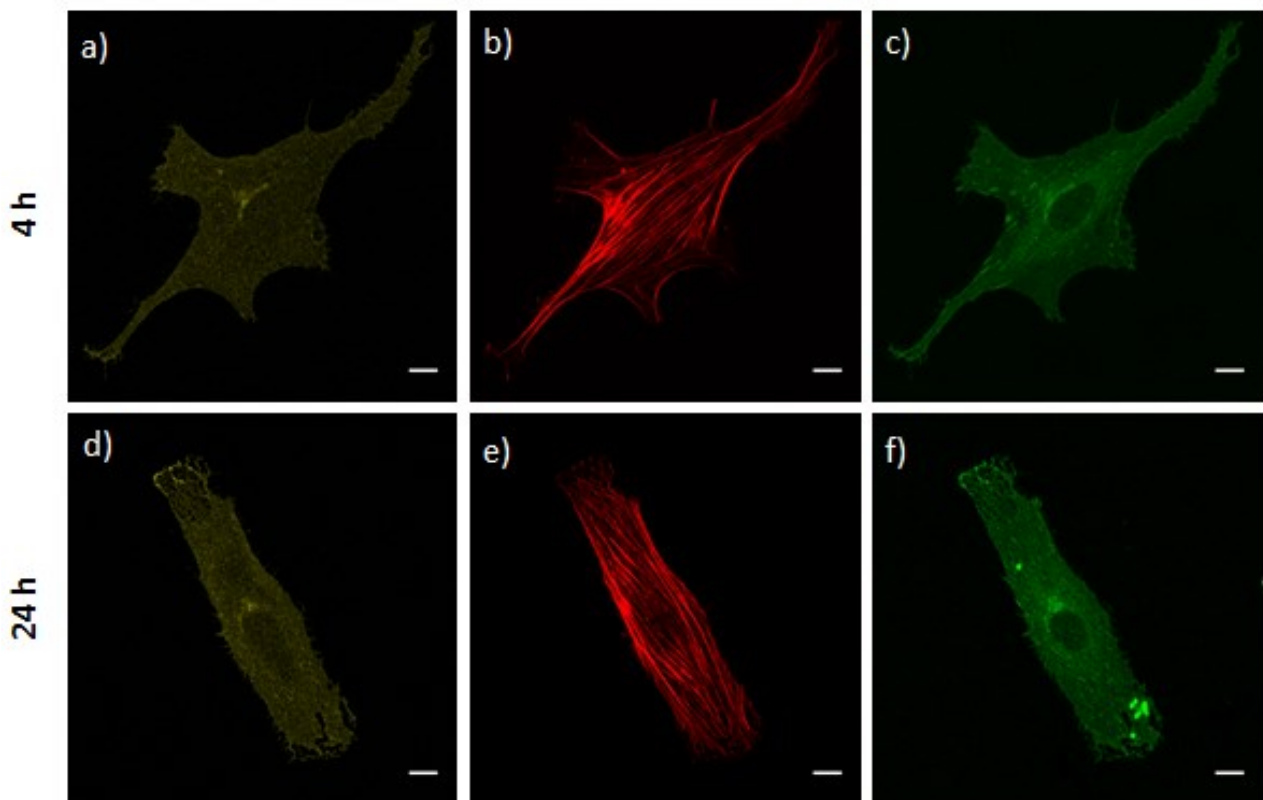
Fig. 1 Confocal microscopy images of single endothelial cells seeded on flat treated surfaces. Intracellular junction were detected through VE- Cadherin (a,d), actin fibers were stained with Alexa Fluor 488 Phalloidin (b,e), FAs were immunostained for vinculin (c,f). Scale bars are 10 μm.

Endothelial cells seeded on flat surfaces at high density expressed VE-cadherin with a spatial arrangement different from what observed in single cell analysis (Fig 2a,d). Additionally, we observed that FAs were more abundant in absence of cadherin (Fig.3). Since both FA and cadherin are both connected to actin fibers [5], it is likely that different arrangement of stress fibers form in multicellular aggregates that alter cell mechanics. Therefore we suggested that the force exerted by the cell-cell junctions was stronger than cell material interaction. Also in this case, z-stacks of confocal images were acquired to study structural architecture of the cytoskeleton. Here, a different assembly of actin fibers was detected. Actin bundles do not cover the whole cell area but were placed in peripheral regions, arranged at the cell edges, away from the nucleus unlike what observed in single cell experiment, in which the actin cytoskeleton wrapped the entire cell nucleus (Fig 2b,e). This phenomenon was even amplified at 24h. In this case cell cytoplasm was devoid of stress fibers which remained anchored at cell periphery (Fig 2e). We hypothesized that due to the remodeling of intercellular junctions and the mechanisms of cell contractility the actin cytoskeleton organization was altered. This hypothesis appeared to be confirmed also by the analysis of mean intensity of fluorescence of phalloidin that showed high levels of fluorescence intensity in isolated cells as they have a structured cytoskeleton, conversely, in cell populations, in presence of extensive cell-cell contacts low levels of fluorescence were recorded because of remodeling mechanisms promoted by cadherins (Fig. 4).
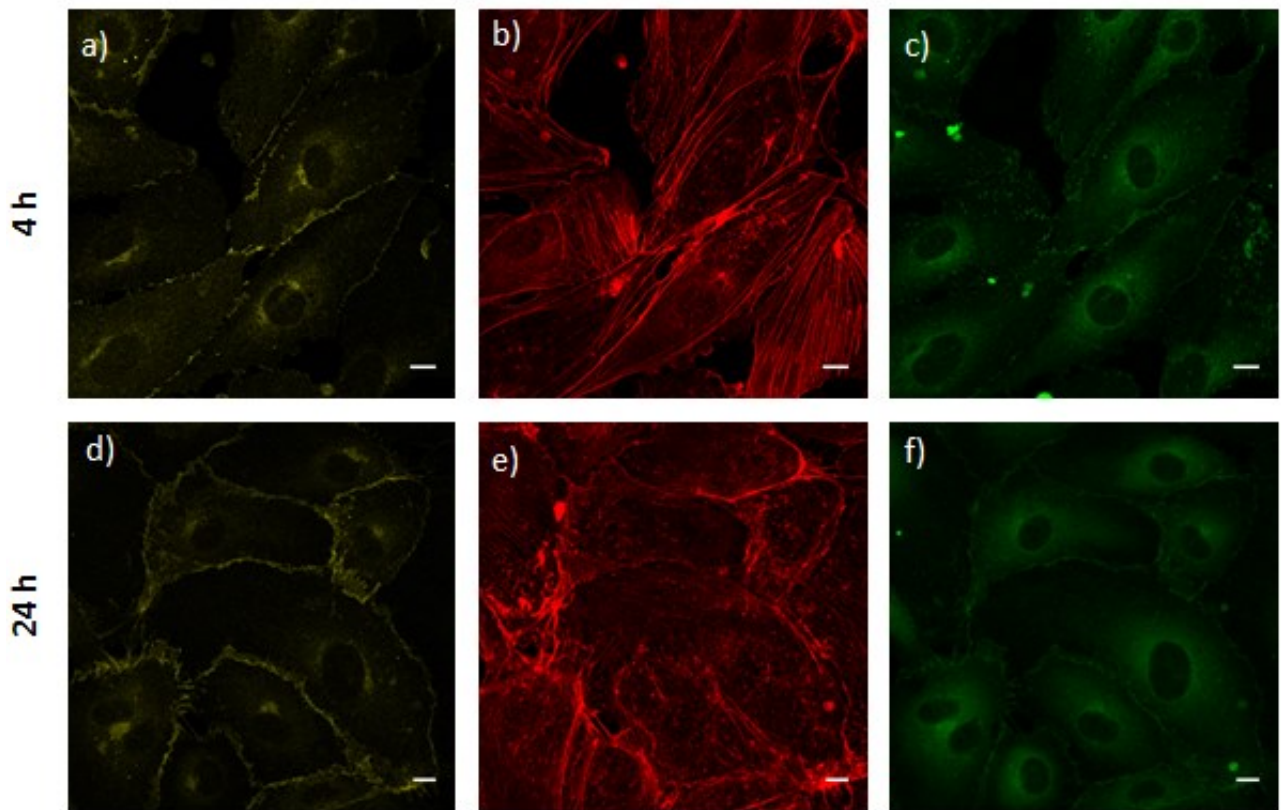
Fig. 2. Confocal microscopy images of confluent endothelial cells seeded on flat treated surfaces. Intracellular junction were detected through VE- Cadherin (a,d), actin fibers were stained with Alexa Fluor 488 Phalloidin (b,e), FAs were immunostained for vinculin (c,f). Scale bars are 10 μm.
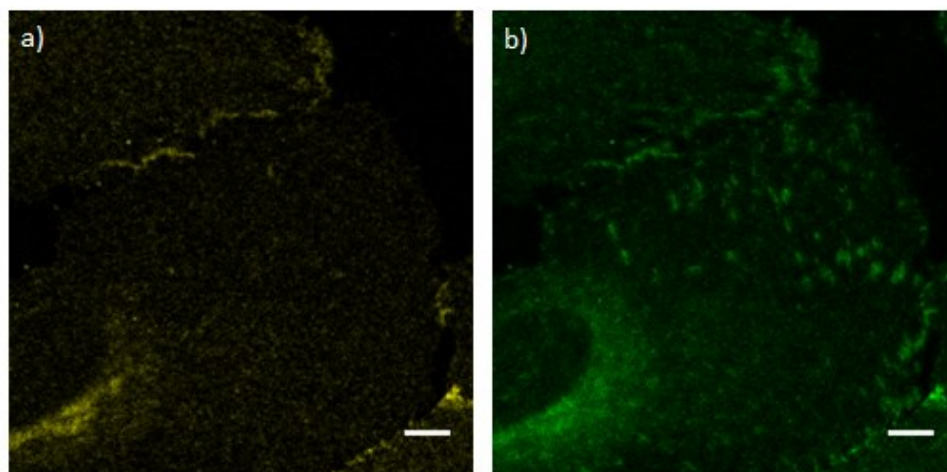
Fig. 3 Confocal images details of confluent endothelial cells seeded on flat treated surfaces. Adherent junctions were visualized with VE-Cadherin (a) and FAs with anti-vinculin antibody (b). Scale bars are 5 μm.
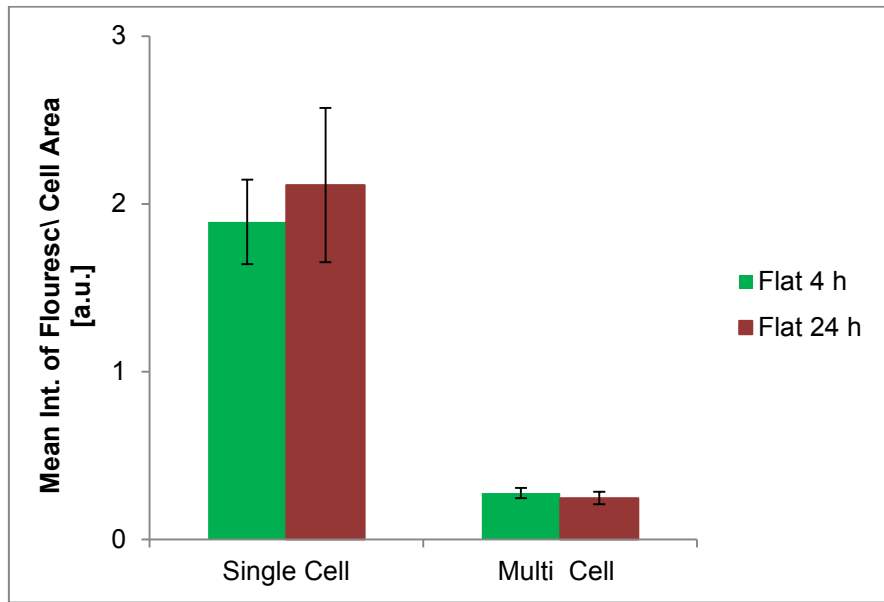
Fig.4 Histogram of normalized mean intensity of fluorescence of phalloidin for the cell area in single cells and in cell populations in presence of cell-cell contact at 4h and 24h. Error bars are s.e.m.

4.2.2. Mechanical Characterization

In order to investigate how the differential assembly of the cytoskeleton caused by cell-cell contacts affected cell mechanic, a through characterization of the mechanical behavior of the cytoplasmic and nuclear region was performed (Fig 4). As regards nuclear region, cells which are in a state of confluence showed lower mechanical properties than cells that are found as single cells. Low nuclear stiffness in confluent cells is due to the fact that in cell populations actin bundles are confined in the cell peripheral area and are subject to the remodeling of the cell-cell junctions, therefore they are not able to exert compressive forces on the nucleus as to increase its mechanical properties. Unlike the single cells in which the actin

cytoskeleton covers the whole cell area and in this way can alter the nuclear tensional state. Also investigations carried out in the cytoplasmic region displayed that confluent cells are softer than single cells, this was due to a cytoskeleton assembly poorer of structured actin, continuously subject to remodeling events by cadherin complex; contrary to the single cells where the actin network is better organized.
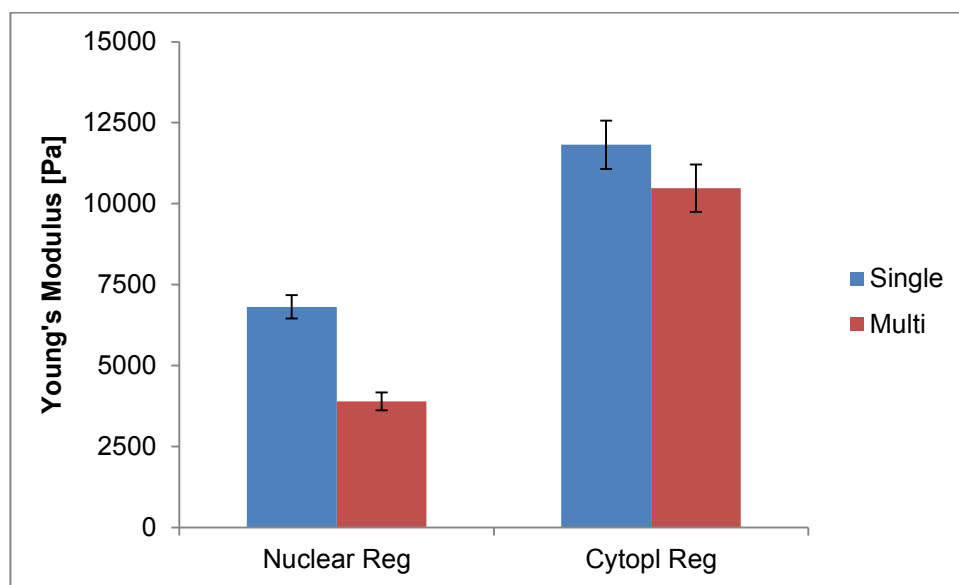
Fig.4 Histogram of mechanical properties of cytoplasmic and nuclear region in single cells and cell populations.

References

1. Giannotta M, Trani M, Dejana E. 2013 VE-Cadherin and Endothelial Adherens Junctions: Active Guardians of Vascular Integrity. Developmental Cell, 26, 441–454 doi:10.1016/j.devcel.2013.08.020

2. Leckband DE, De Rooij J. 2014 Cadherin Adhesion and Mechanotransduction. 2014 Cell and Developmental Biology 30, 291-315 doi: 10.1146/annurev-cellbio-100913-013212

3. Liu Z, Tan JL, Cohen DM, Yang MT, Sniadecki NJ, Ruiz SA, Nelson CM, Chen CS. 2010 Mechanical tugging force regulates the size of cell-cell junctions. Proc. Natl. Acad. Sci. Usa 107,9944-49

4. Ladoux B, Anon E, Lambert M, Rabodzey A, Hersen P, Buguin A, Silberzan P, Mège R. 2010 Strength Dependence of Cadherin-Mediated Adhesions. Biophysical journal 98, 534-542

5. Yonemura S. 2011. Cadherin–actin interactions at adherens junctions. Current Opinion in Cell Biology. 23:515–522 DOI 10.1016/j.ceb.2011.07.001

CHAPTER 5

CONCLUSIONS

In Mechanobiology is recognized the role of exogenous signals displayed by biomaterials in influencing the cell fate and function. It was recently seen that biophysical signals in the form of mechanical signals or cell shape constraints through topographic or adhesive islands have a powerful effect in altering cellular behavior such as migration, proliferation and differentiation [1]. The differentiation process is very relevant in applications such as regenerative medicine or tissue engineering, which aim at developing strategies for the stem cells differentiation using minimal amounts of biochemical signals that can elicit adverse effects to the host organism. Literature works highlighted that the adhesive processes and the development of a given actin cytoskeleton are essential in dictating the cell fate [2]. The aim of my thesis was to engineer nanopatternated platforms in order to govern not only adhesive processes but also cellular mechanics. This acquires a central relevance to understand how adhesiveness and cytoskeleton assemblies could influence cell and nuclear morphology along with their mechanical responses. The results obtained suggest that the designed nanopatterning and biochemical functionalization alter FA shape that impacts stress fiber assembly and contractility. Since stress fibers might be directly connected to the nuclear envelope and might transfer on this compressive forces, it is likely that stress fibers can deform the nucleus through myosin contraction. We demonstrated that this process is particularly evident on nanopatterned substrates, here parallel arrays of actin bundles exert a coordinated action on the nucleus. We moved forward and showed that lamins A\C have a primary role in dictating the mechanical properties of the nuclear region. These results may be relevant for the translation of gene signals and the expression of specific proteins.

Later, we investigated how in cell populations, the presence of extensive cell-cell contacts could alter the cytoskeleton morphology and consequently the cytoskeleton and nuclear mechanics. The investigations we carried out, showed that individual cells displayed high mechanical properties, in particular for the nuclear region, whereas when there is a cell-cell contact actin is redistributed in the cortical area, freeing the nucleus, which exhibits different mechanical conformations characterized by lower moduli.

Overall, these results could have great relevance in mechanotransduction processes of endothelial cells and in application contexts where these cells must keep a given differentiation state, which requires adequate stress states. Therefore, in order to engineer devices to maintain the right differentiation of endothelial cells it is required to take account not only of the cues displayed by the material but also the signal that cells exchange between them.

References

1. Ventre M, Netti PA. 2015. Engineering Cell Instructive Materials To Control Cell Fate and Functions through Material Cues and Surface Patterning. ACS Appl. Mater. Interfaces. DOI: 10.1021/acsami.5b08658

2. Lee J, Abdeen A, Kim AS, Kilian KA. 2015. Influence of Biophysical Parameters on Maintaining the Mesenchymal Stem Cell Phenotype. ACS Biomater. Sci. Eng. 1, 218–226. DOI: 10.1021/ab500003s
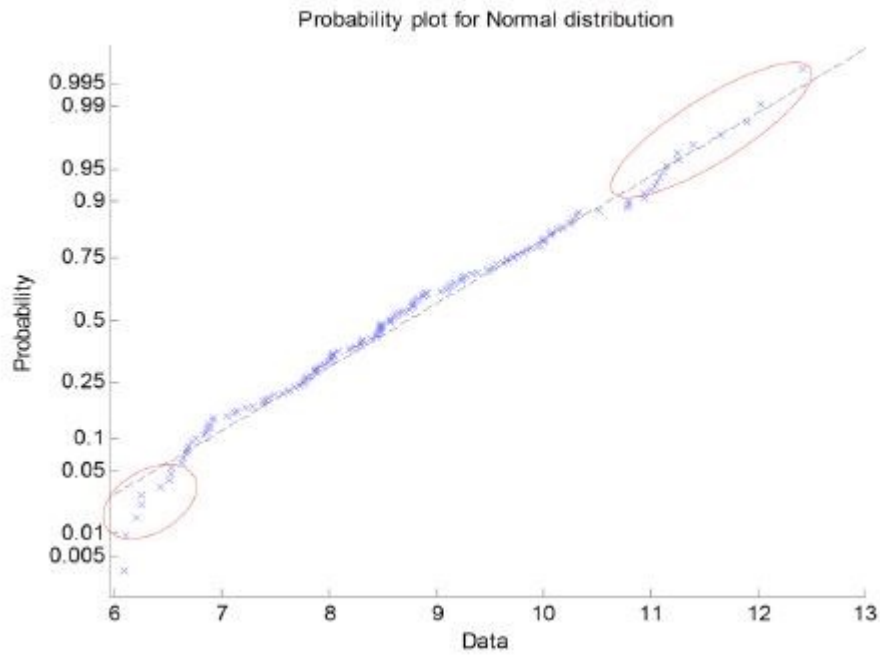
Appendix A
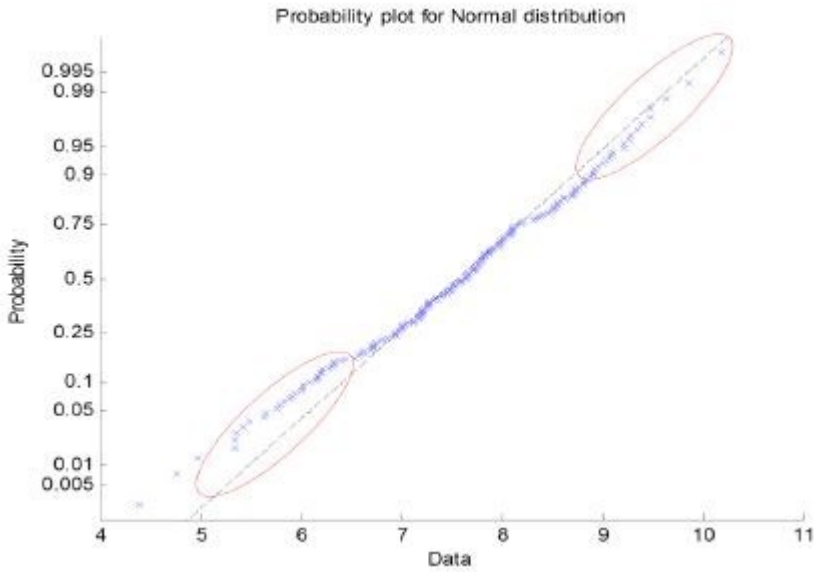
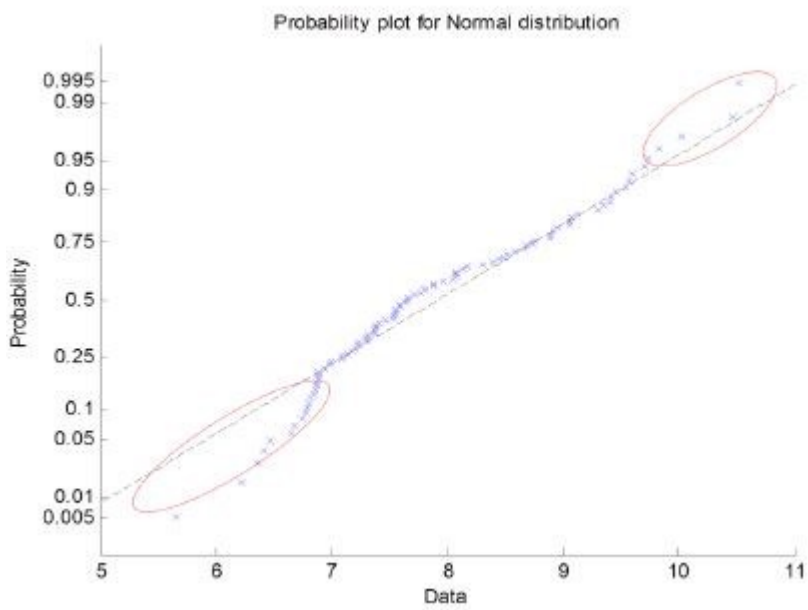Fig. A1 Probability Plot 100nm cell body hMsc 700nm Pt FN
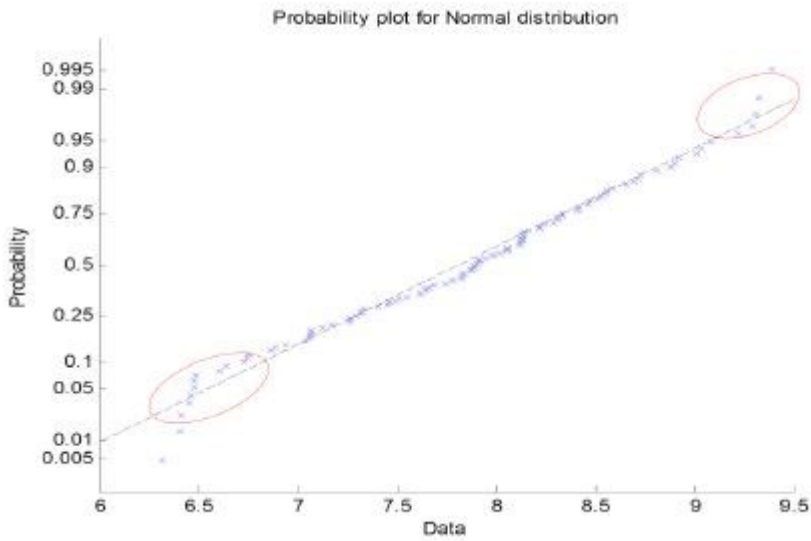
Fig. A2 Probability Plot 200nm nuclear region hMsc 700nm Pt FN
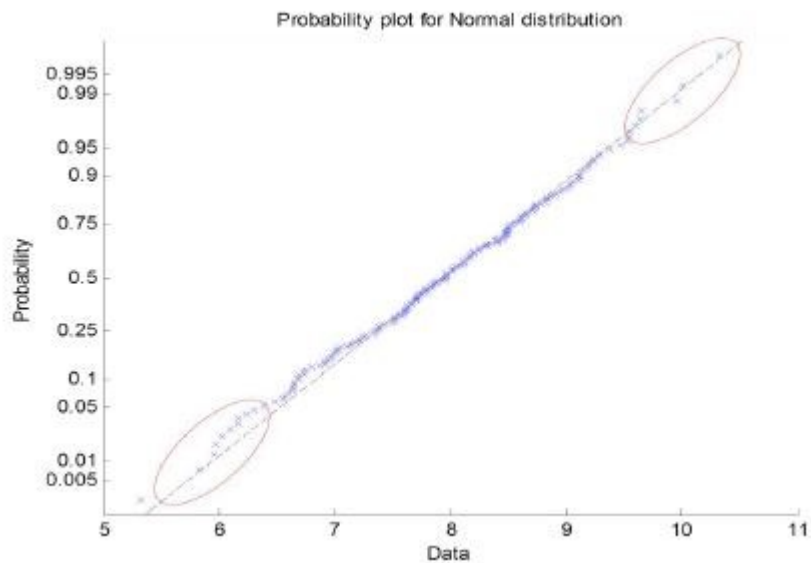
Fig. A3 Probability Plot 200nm cell body hMsc 700nm Pt FN
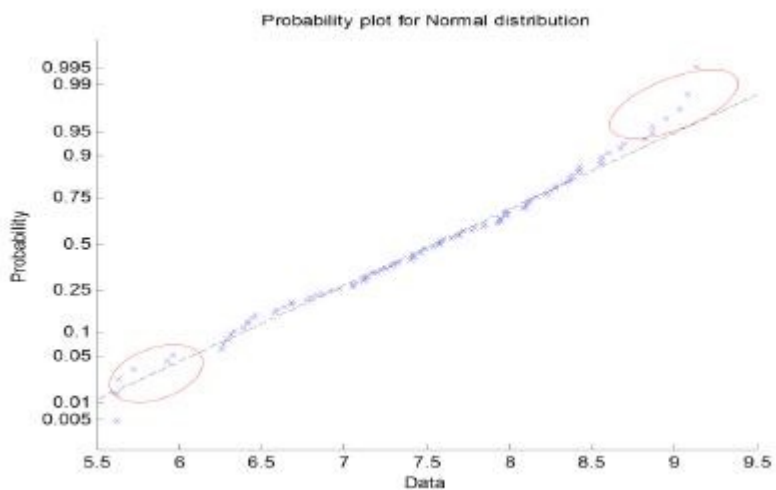
Fig. A4 Probability Plot 400nm nuclear region hMsc 700nm Pt FN
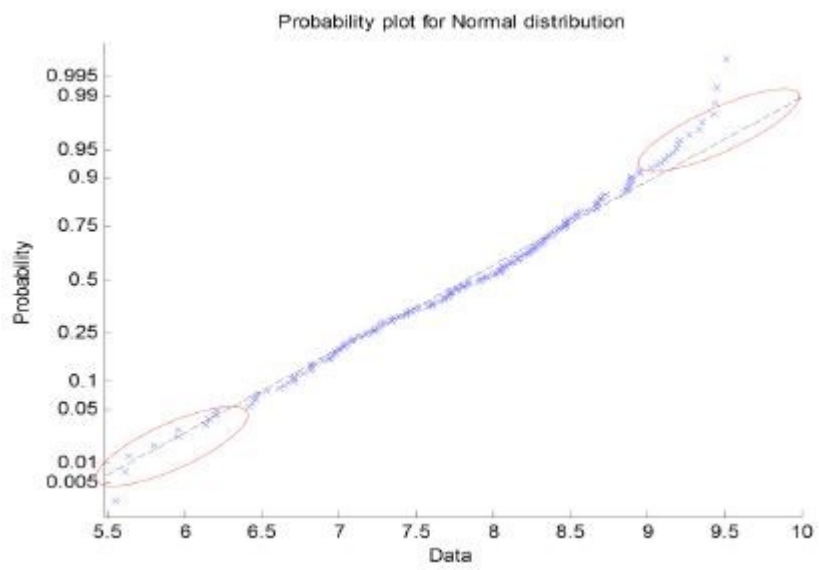
Fig. A5 Probability Plot 400nm cell body hMsc 700nm Pt FN
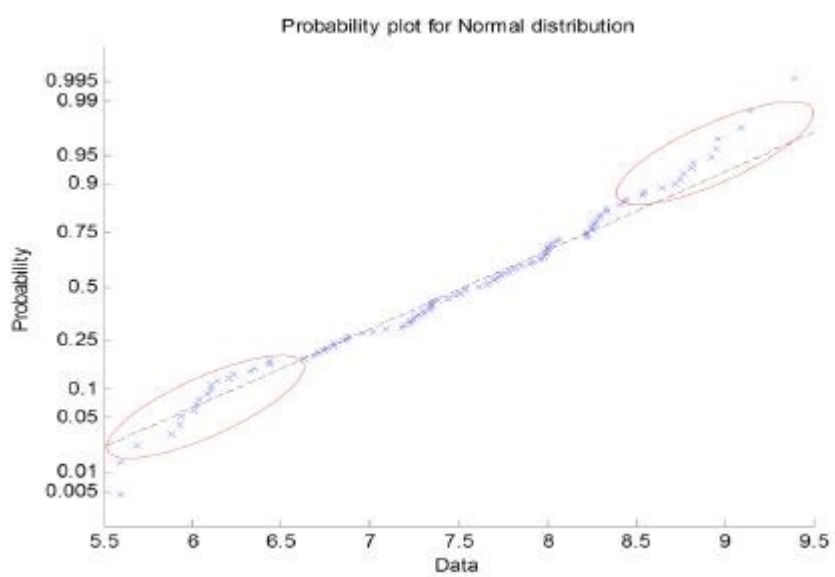
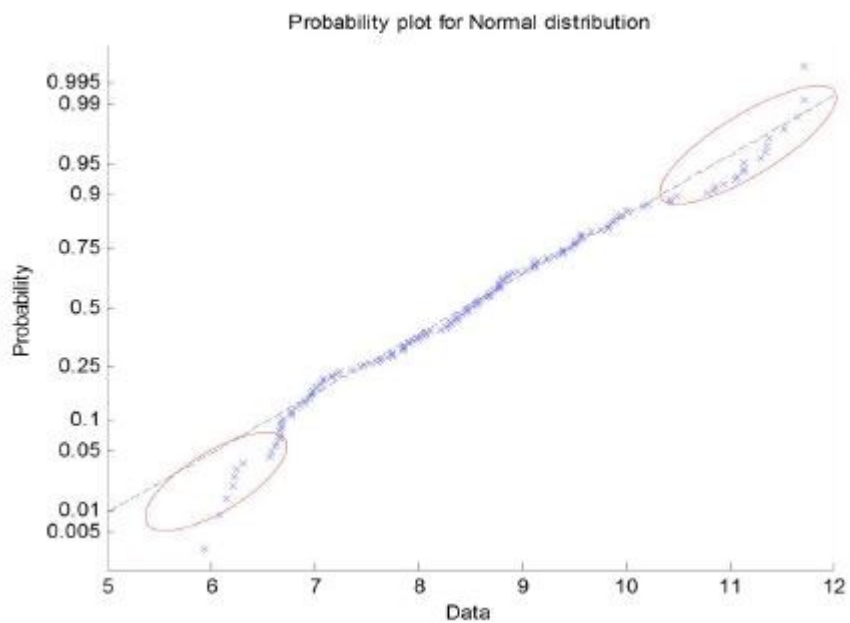Fig. A6 Probability Plot 500nm nuclear region hMsc 700nm Pt FN
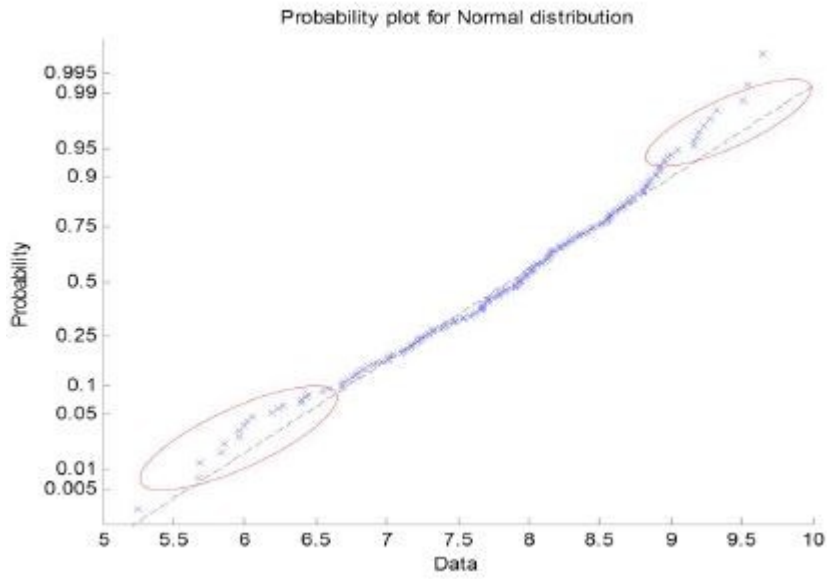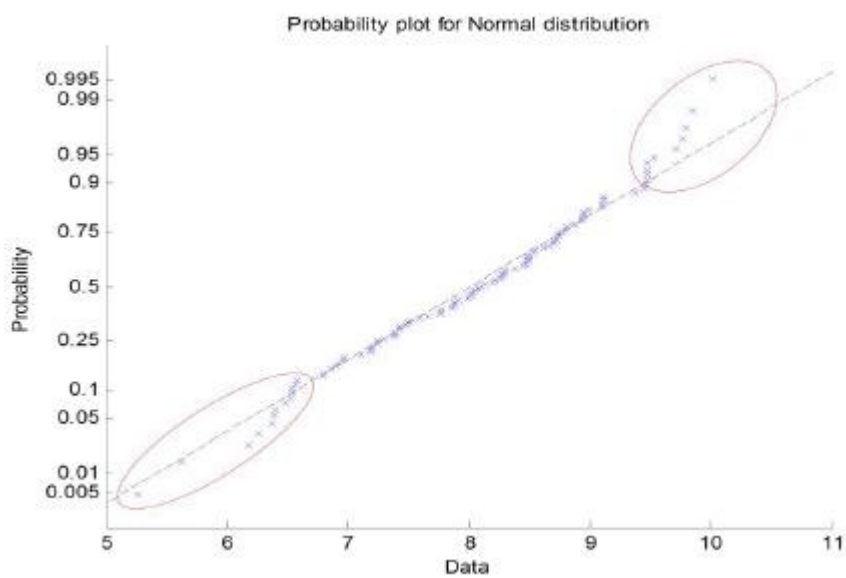
Fig. A7 Probability Plot 500nm cell body hMsc 700nm Pt FN
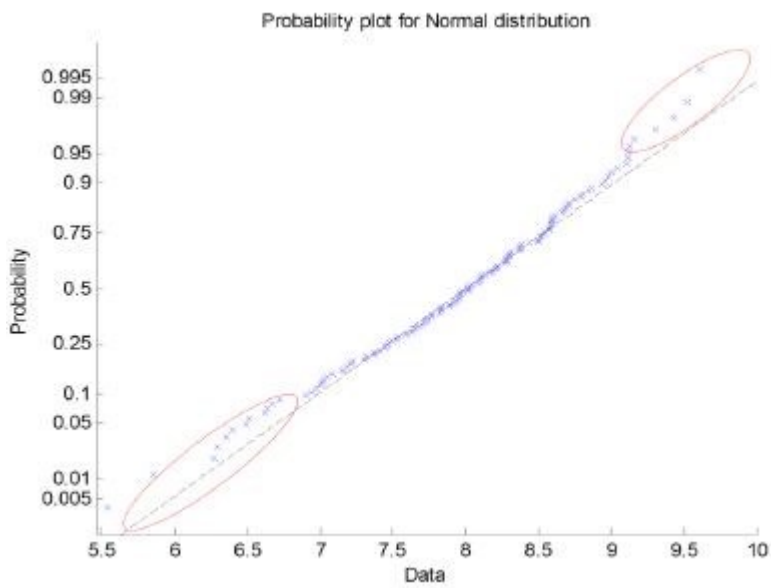
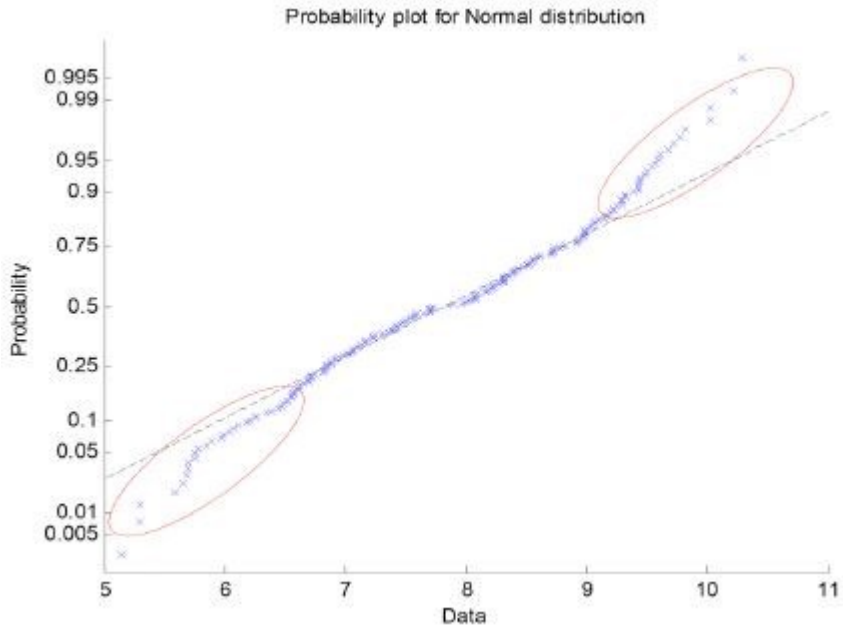Fig. A8 Probability Plot 100nm nuclear region hMsc FLAT Pt FN
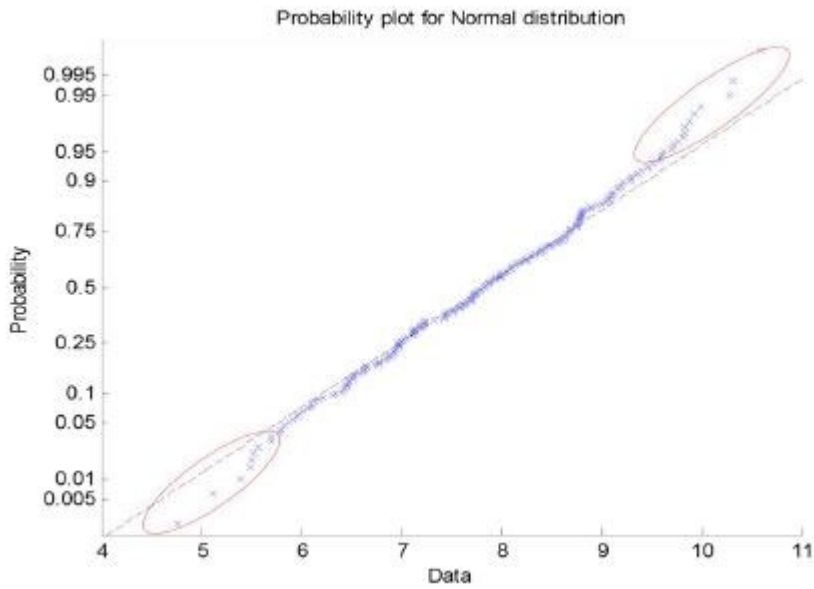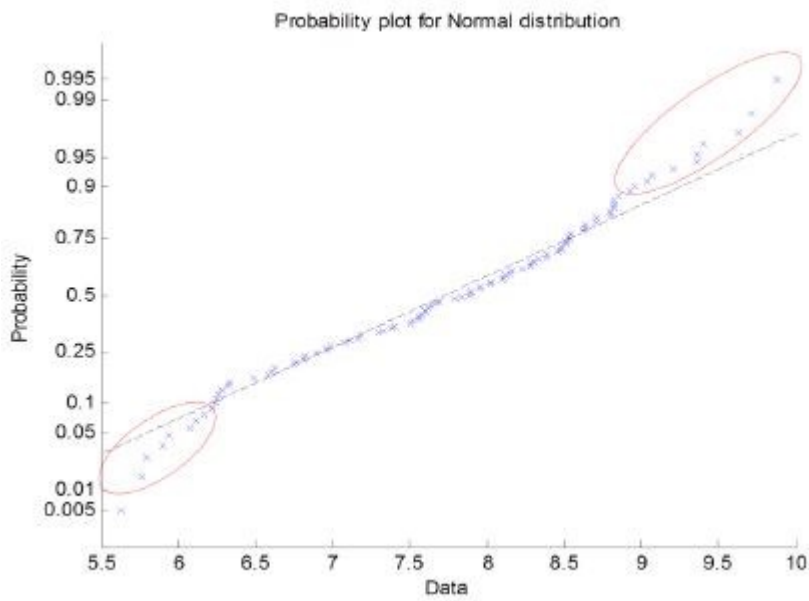
Fig. A9 Probability Plot 100nm cell body hMsc FLAT Pt FN
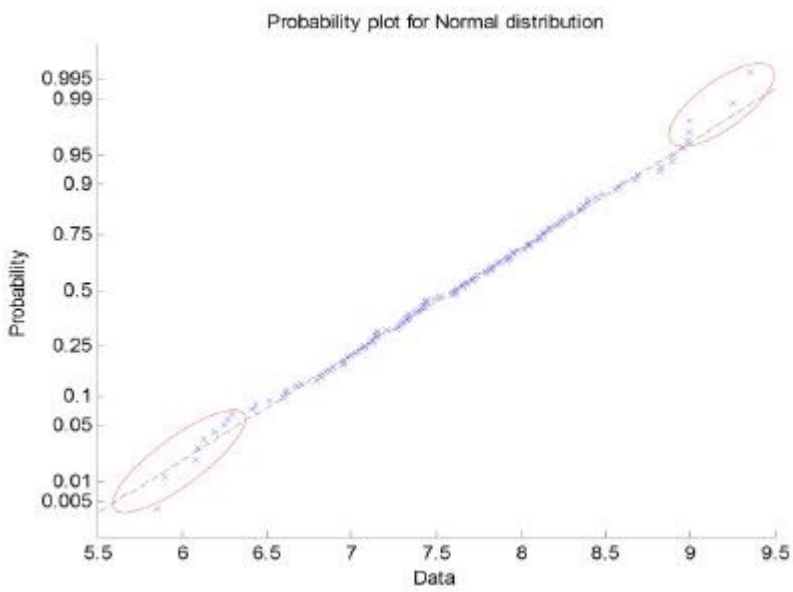
Fig. A10 Probability Plot 200nm nuclear region hMsc FLAT Pt FN
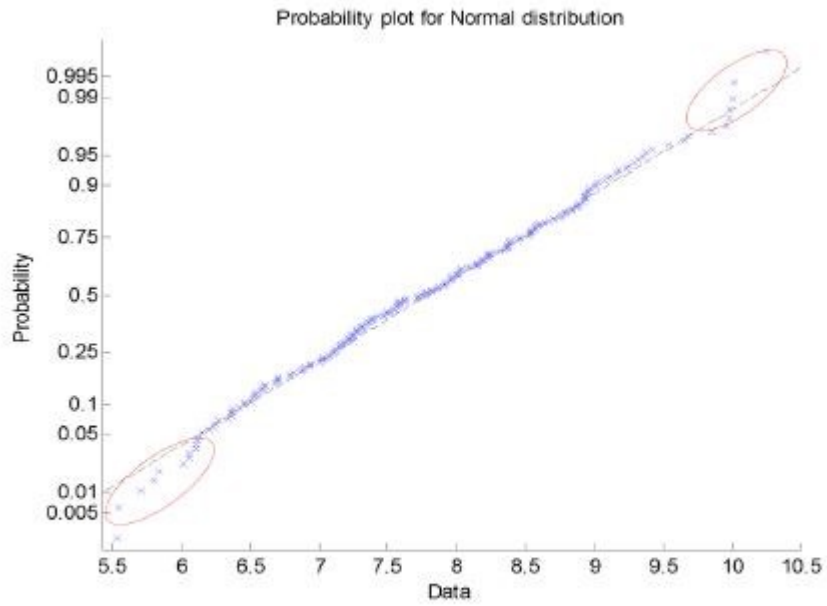
Figura 24: ProbPlot 200 nm corpo cellulare FN Flat

Fig. A11 Probability Plot 200nm cell body hMsc FLAT Pt FN
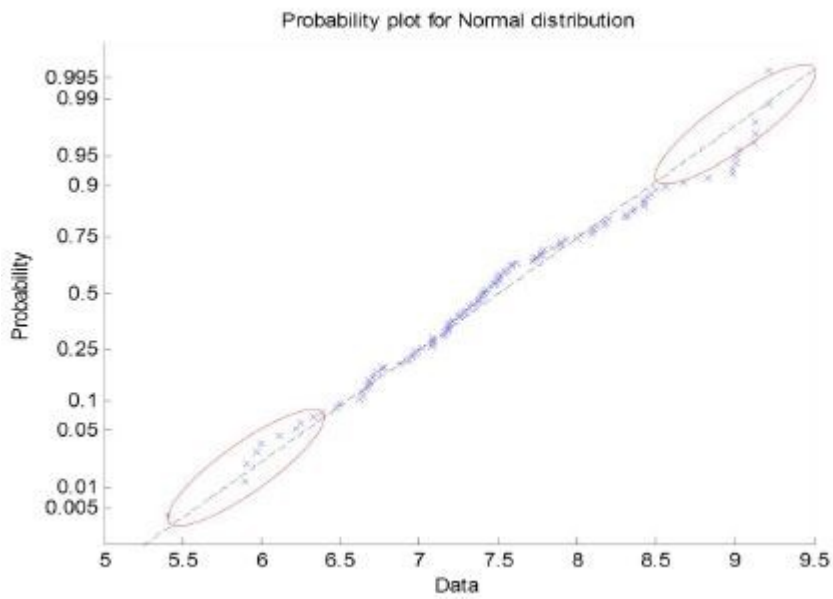
Fig. A12 Probability Plot 400nm nuclear region hMsc FLAT Pt FN
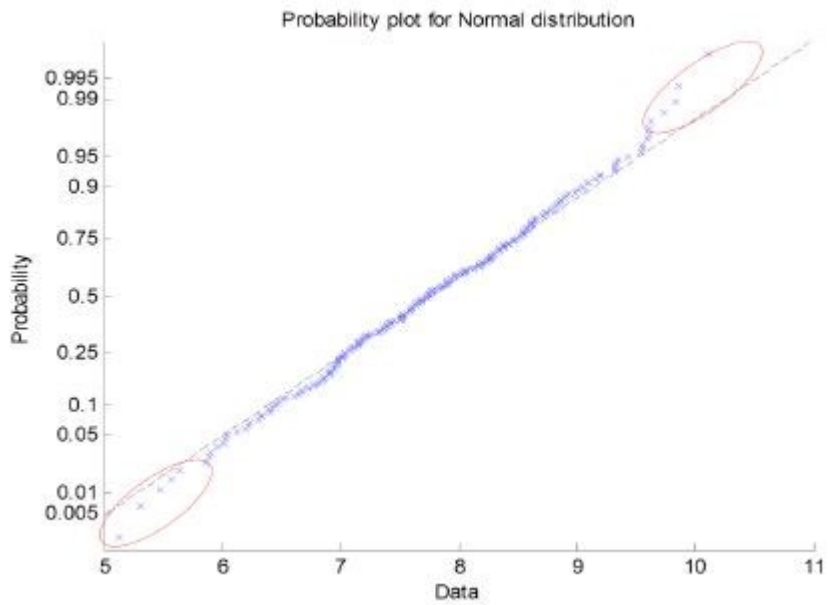
Fig. A13 Probability Plot 400nm cell body hMsc FLAT Pt FN
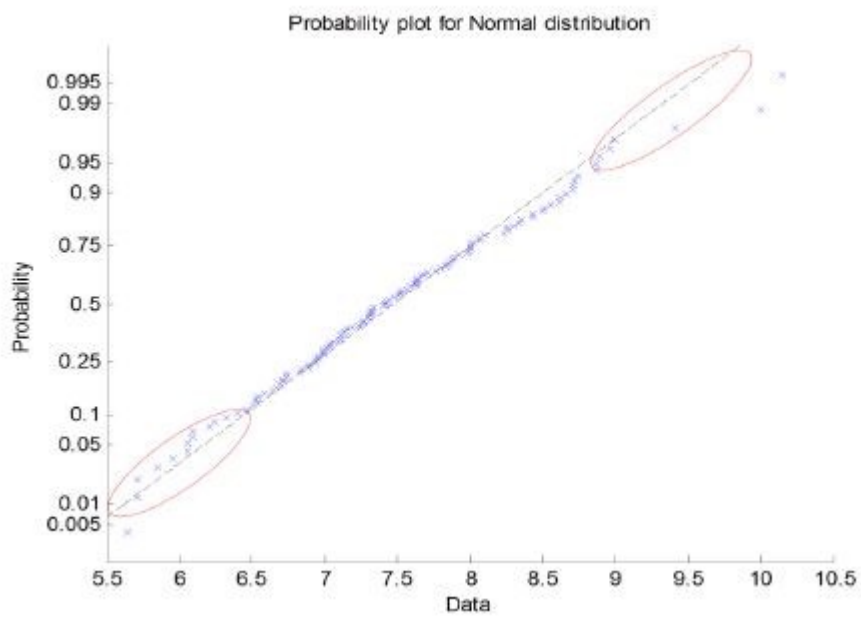
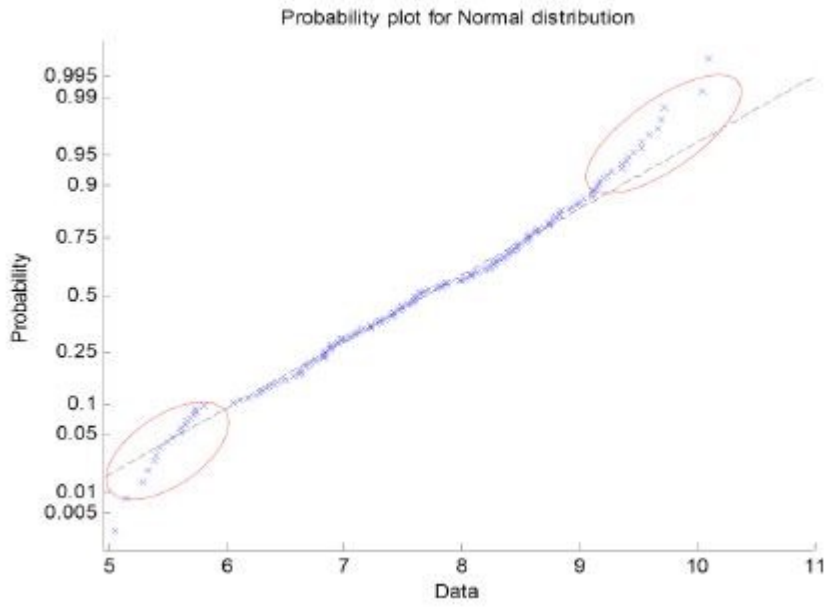Fig. A14 Probability Plot 500nm nuclear region hMsc FLAT Pt FN
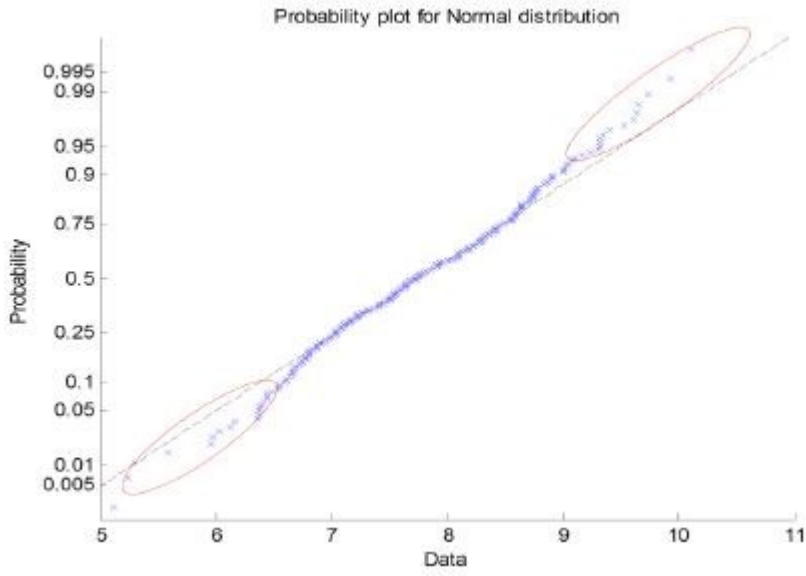
Fig. A15 Probability Plot 500nm cell body hMsc Flat Pt FN
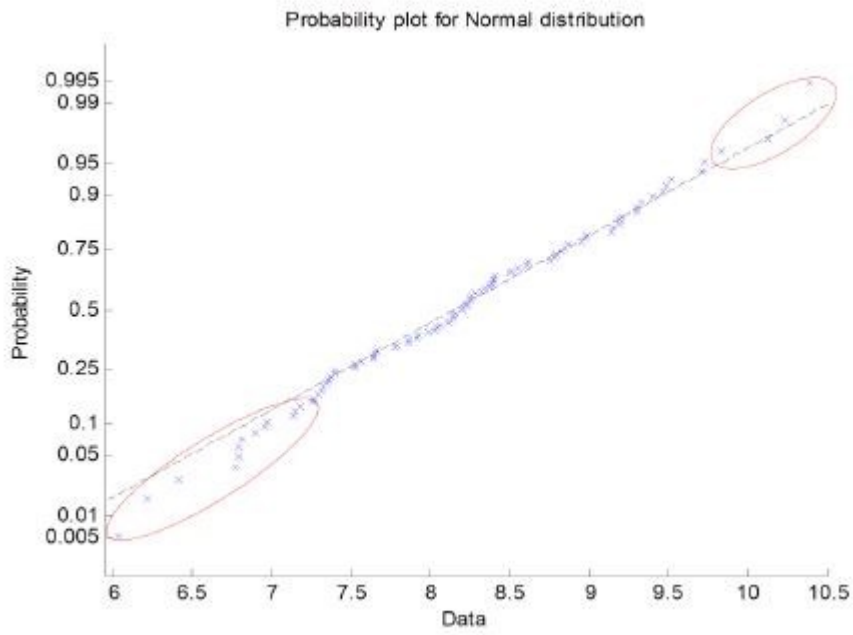
Fig. A16 Probability Plot 100nm nuclear region hMsc 700nm Pt FBS
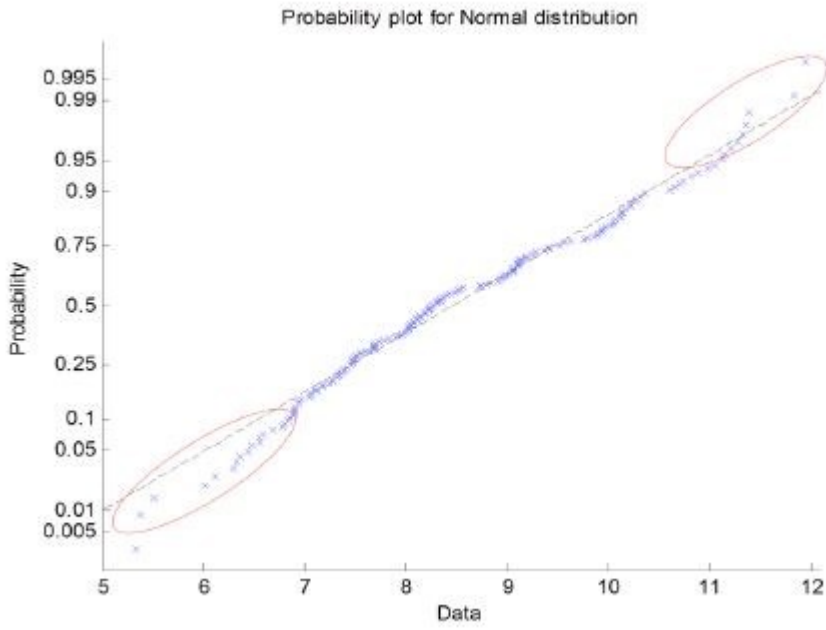
Fig. A17 Probability Plot 100nm cell body hMsc 700nm Pt FBS
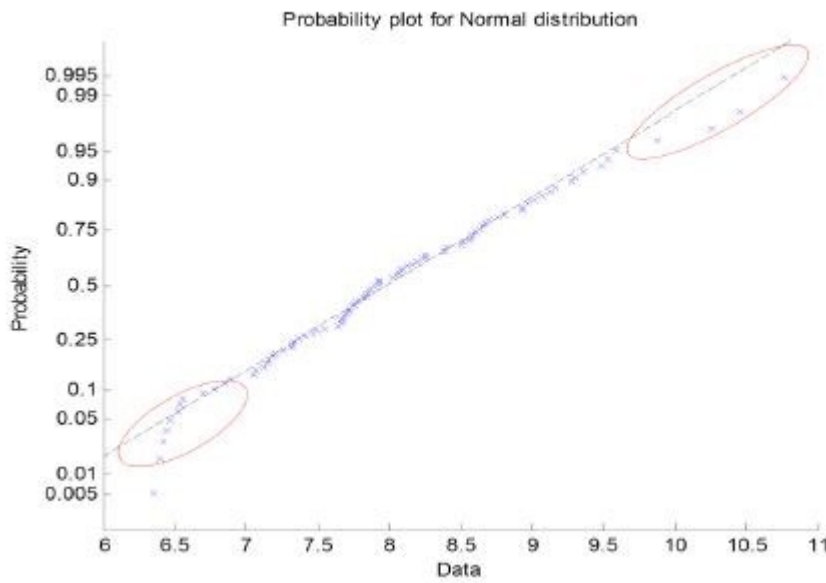
Fig. A18 Probability Plot 200nm nuclear region hMsc 700nm Pt FBS
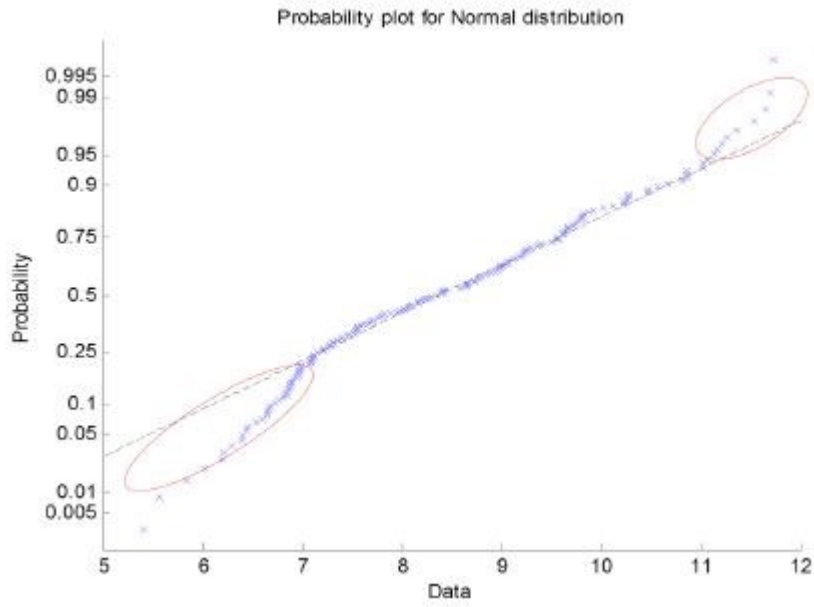
Fig. A19 Probability Plot 200nm cell body hMsc 700nm Pt FBS
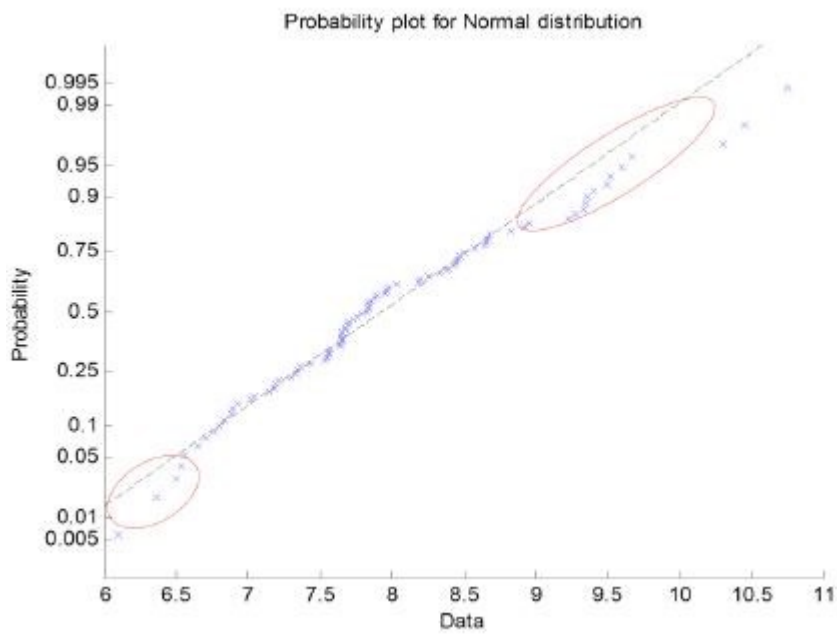
Fig. A20 Probability Plot 400nm nuclear region hMsc 700nm Pt FBS

Fig. A21 Probability Plot 400nm cell body hMsc 700nm Pt FBS

Fig. A22 Probability Plot 500nm nuclear region hMsc 700nm Pt FBS

Fig. A23 Probability Plot 500nm cell body hMsc 700nm Pt FBS

Fig. A24 Probability Plot 100nm nuclear region hMsc FLAT Pt FBS
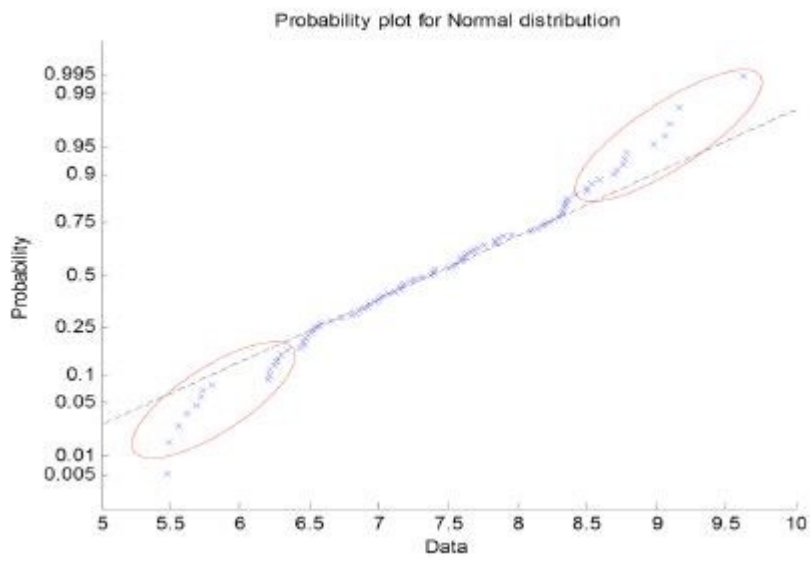
Fig. A25 Probability Plot 100nm cell body hMsc FLAT Pt FBS

Fig. A26 Probability Plot 200nm nuclear region hMsc FLAT Pt FBS

Fig. A27 Probability Plot 200nm cell body hMsc FLAT Pt FBS

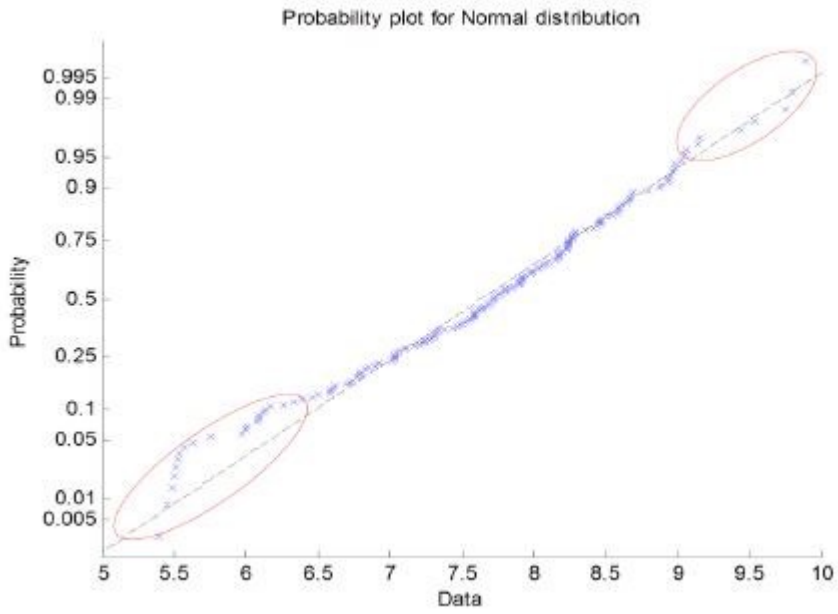Fig. A28 Probability Plot 400nm nuclear region hMsc FLAT Pt FBS

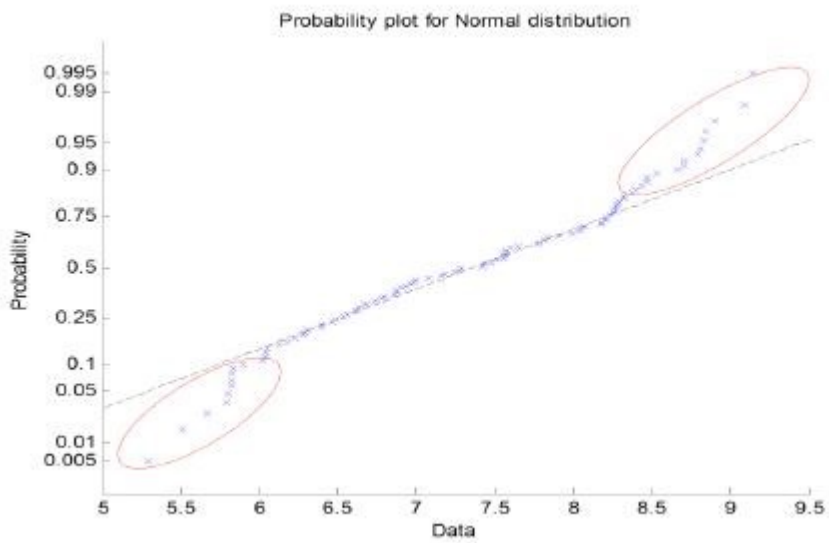Fig. A29 Probability Plot 400nm cell body hMsc FLAT Pt FBS

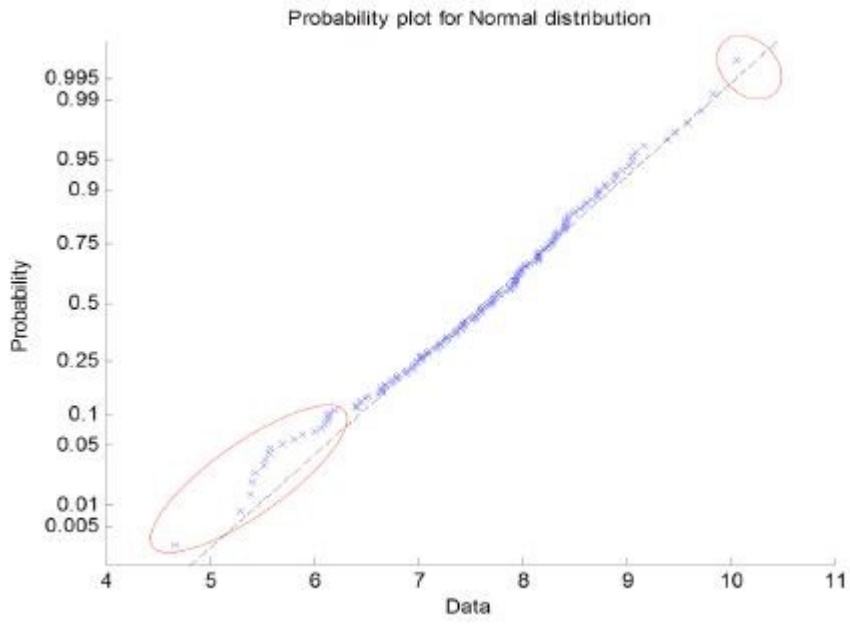Fig. A30 Probability Plot 500nm nuclear region hMsc FLAT Pt FBS

Fig. A31 Probability Plot 500nm cell body hMsc FLAT Pt FBS